Czech Technical University in Prague

Faculty of Electrical Engineering

Department of Telecommunication Engineering

Master Thesis

Non-linear Four-wave Mixing in DWDM Systems

Author: BSc. Aldair da Costa Baptista

Supervisor: Ing. Michal Lucki, Ph.D.

MASTER'S THESIS ASSIGNMENT

I. Personal and study details

Student's name: **Baptista Aldair da Costa** Personal ID number: **453308**

Faculty / Institute: **Faculty of Electrical Engineering**

Department / Institute: **Department of Telecommunications Engineering**

Study program: **Electronics and Communications**

Specialisation: **Communication Systems and Networks**

II. Master's thesis details

Master's thesis title in English:

Non-linear Four-wave Mixing in DWDM Systems

Master's thesis title in Czech:

Nelineární čtyřvlnné směšování u DWDM systémů

Guidelines:

The goal of this work is to model the phenomenon of four-wave mixing (FWM) in optical networks and to create a laboratory experiment that confirms theoretical predictions. A partial goal is to investigate the effect of the four-wave mixing effect (its options) on selected optical networks using dense wavelength multiplexing and optoelectronic amplifiers. Another objective is to investigate the combination of FWM phenomenon with other destructive factors such as dispersion, attenuation, wrong channel spacing or unsuitable modulations. Perform the simulations in Optsim environment and use the ITU-T recommendations in this area. The next goal is an experiment - excitation of FWM in a fibre coil with some near-zero dispersion, using available lasers, fibres and spectral analyser. Comparison experimental results with simulations and previous works. Finally yet importantly, propose an efficient method of suppressing or eliminating the FWM in DWDM networks.

Bibliography / sources:

[1] Agrawal, G.P.: Lightwave Technology: Telecommunication Systems, Wiley Interscience, USA, New Jersey, 2005. ISBN: 978-0-471-21572-1.
[2] Freude, W.; Schmogrow, R.: Quality Metrics for Optical Signals: Eye Diagram, Q-factor, OSNR, EVM and BER, in Proceedings of 14th International Conference on Transparent Optical Networks, Coventry, England, paper Mo.B1.5, 2012.
[3] ITU-T G-series Supplement 39: Transmission systems and media, digital systems and networks. ITU, 2012. Dostupné na http://www.itu.int/rec/T-REC/en [on-line]

Name and workplace of master's thesis supervisor:

Ing. Michal Lucki, Ph.D., Department of Telecommunications Engineering, FEE

Name and workplace of second master's thesis supervisor or consultant:

Date of master's thesis assignment: **08.01.2020** Deadline for master's thesis submission: **14.08.2020**

Assignment valid until: **30.09.2021**

Ing. Michal Lucki, Ph.D. Supervisor's signature	Head of department's signature	prof. Mgr. Petr Páta, Ph.D. Dean's signature

III. Assignment receipt

The student acknowledges that the master's thesis is an individual work. The student must produce his thesis without the assistance of others, with the exception of provided consultations. Within the master's thesis, the author must state the names of consultants and include a list of references.

. _____ Date of assignment receipt

_____ Student's signature

Declaration

I hereby declare that I am the sole author of the thesis entitled "Non-linear Four-wave Mixing in DWDM Systems " and all the duly references and quotations have been marked in the respective list of references, under carefully supervision of my thesis supervisor. This declaration also extends the consent of publishing my work with the correspondent department licensing.

In Prague on 13th August 2020 Signature

Acknowledgements

First and foremost, I would like to thank God almighty for his grace and countless love.

I wish to express my sincere appreciation and gratitude to the supervisor of my thesis, Ing. Michal Lucki, Ph.D. for the necessary guidance and assistant in producing this work, rest to say we come a long way.

To all relatives, friends, faculty colleagues, and all the other people whose names I did not mention but contributed directly or indirectly to this work I would like to express my gratitude.

A todos o meu muito obrigado em especial o pessoal do "Regimento" !

Abstract

The study object of this master's thesis is to study a non-linear phenomenon called four waver mixing, its causes and consequences and how to mitigate its effect, all within the context of optical networks with spacings of dense channels. Throughout this work, typified rules were applied within the standards of the international telecommunications association (ITU) and in some cases the system was put to the test by extending the tolerance of certain factors.

The proposed work environment houses a simulator with characteristics very close to those found during the design of optical networks. At first sight, several experiments were carried out in this simulator in order to appear FWM, and later for a controlled experimental lab environment. The practical experiments were conducted with the same scientific rigor applied to the simulator with an emphasis on non-degenerated FWM typification.

Keywords: optical networks, nonlinear effects, four wave mixing, DWDM systems, optical fibers, optical laser sources, optical amplifiers, Optsim Simulator, Experimental, signal multiplexing.

Abstrakt

Cílem této diplomové práce je studovat nelineární jev zvaný míchání čtyřmi vlnami, jeho příčiny a důsledky a jak zmírnit jeho účinek, a to vše v kontextu optických sítí s rozestupy hustých kanálů. Během této práce byla aplikována typizovaná pravidla v rámci standardů Mezinárodní telekomunikační asociace (ITU) a v některých případech byl systém testován rozšířením tolerance určitých faktorů.

Navrhované pracovní prostředí obsahuje simulátor s charakteristikami velmi blízkými těm, které byly nalezeny při návrhu optických sítí. Na první pohled bylo v tomto simulátoru provedeno několik experimentů, aby se objevil FWM, a později pro kontrolované experimentální laboratorní prostředí. Praktické experimenty byly prováděny se stejnou vědeckou přísností jako na simulátoru s důrazem na nedegenerovanou typificace FWM.

Klíčová slova: optické sítě, nelineární jevy, míchání čtyř vln, systémy DWDM, optická vlákna, zdroje optického laseru, optické zesilovače, simulátor Optsim, experimentální, multiplexování signálu.

Contents

Figure List

Table List

List of abbreviations

BER	Bit Error Rate
XPM	Cross Phase Modulation
DWDM	Dense Wavelength Division Multiplex
EDFA	Erbium Doped fiber amplifier
FDSS	Frequency Domain Split Step
FIR	Finite Impulse Response
FWM	Four-Wave Mixing
GaAs	Gallium Arsenide
LED	Light Emitting Diode
LWP	Low Water Peak “Fibers”
MAN	Metropolitan Area Network
NLSE	Nonlinear Schrodinger Equation
NZ-DSF	Non-Zero Dispersion Shifted Fibers
OSNR	Optical Signal-To-Noise Ratio
PDH	Plesiochronous Digital Hierarchy
PN	Positive Negative “P-type N-type junction”
QoS	Quality of Service
SBS	Stimulated Brillouin-Scattering
SDH	Synchronous Digital Hierarchy
SPM	Self Phase Modulation
SRS	Stimulated Raman Scattering
SSFM	Split Step Fourier Method
TDSS	Time Domain Split Step
WDM	Wavelength Division Multiplexing

1. Introduction

In this work, the researcher focuses primarily on optical communication systems. The first optical telegraph of Claude Chappe was already overlooked by more reliable electrical telecommunications system with the invention of the laser was more than six decades ago. The first part of an equation was already there notwithstanding that scientists had not yet found a way of utilizing the laser light for optical communication. Another early constraint was the optical fibers had high losses (around 10% of light travelled the fiber). Adjustments were made, mainly on the component of the core and the change from micro-waves to optical waves (modulation still need it). More recently first generations systems were designed. These systems theoretically operated at a bit rate of 45 Mbit/s in the near-infrared spectral region. This is because the GaAs emit light at wavelengths near 850 nm. A repeater also was part of the scheme since the fiber loss at the wavelength was close to 3dB/km. With this and other techniques to come, data transmission was improved, and waste of bandwidth was avoided [1].

With this was born the wavelength-division multiplexing (WDM) technique. The technique consists of transmitting multiple channels on different wavelengths in a common fiber adopted as the standard of long transmitting capacity at the right cost and being further exploited due to the growing demand on business multimedia applications. Traditionally, WDM systems operating on a bit rate within 10Gb/s were limited to amplitude modulators (only). The scheme alone tends to indicate sensitivity on the receptor end which cannot support 40Gb/s transmissions without combining other modulation techniques and digital processing, code error detection leading to the standardization of the 100Gb/s transmitters. If one follows this perspective, it can be noted that the high demand is not the only factor that makes the users deploy this technology. There are infrastructure costs implicit on long-distance transmission systems and equipment (the ones with SDH support, PDH, IP, frame relay and other hierarchies). These can be significantly reduced with the use of WDM systems combine with optical amplifiers.

The approach to the theme will involve the creation of an experimental model of the FWM effect that will serve to validate the theoretical preconceptions. The other no less important objectives will be to characterize and investigate this phenomenon within optical networks using a dense channel spacing focusing on its behavior when associated to the most diverse factors (attenuation, dispersion) and the effects caused when compared to the quality of the transmission affected to the signal quality, keeping the signal purely optical in the physical layer. This setup will certainly accumulate

degradations along the path traveled by the signal, registering an important metrics for improving and characterizing of the network. The most basic dependencies of this nonlinear effect of four-wave mixing will be observed as the dispersion of the fiber in the transmission region, the separation of channels, and their potential, while using a systematic approach the results obtained are to be compared with the standards in the area and to explore methods that aim to suppress this effect.

1.1. Thesis arrangement

The introductory part of the current work begins with a narrative of historical facts that contributed to the development and implementation of WDM systems. This leads on to the following chapter which includes basics of optical communication going further into different WDW systems and focusing in DWDM systems their formulation and State of the Art. The II Chapter a brief introduction of other linear phenomena where given necessary to establish a difference between the focus of this work. Progressing into III Chapter the FWM was described in detail including an analytical derivation process ending the chapter with common techniques used to supress this phenomenon.

The IV Chapter includes information regarding the components used in the simulation process, from the description of the software used to the description of the metrics used for quality control. The V and VI chapters, which seem to be the most important among the others, contain information derived in order to prove everything discussed in this work, these two chapters were instrumental in order to prove the theoretical foundation on DWDM networks and the FWM problematic.

2. Chapter I — Optical Communication and WDM systems

A generic optical communication system is composed by an optical transmitter a communication channel and an optical receiver. This system is designed to move information from one end to the other one. This type of communication system has a transmission that is not 100% dependent on its core technology. This means there is still a need for auxiliary circuits as it is not yet directly implemented (electrical feed of data). As the names suggest, their functions, are responsible for transmitting the electrical feed of data linked to the transmission circuit in which is converted to light signal with the help of a lighting source such as an LED or a laser in which the amplitude, frequency and phase is meticulously checked to ensure a stable transmission (steady level of fluctuations among these components) and with the help of photodetector and auxiliary circuits in which the input data is recovered.

Depending on the application, LEDs are typically used for shorter distances and in scenarios that do not require a high data transmission and with low energy capacity. For higher distances, it is necessary to use lasers. Those lasers are more sensitive to changes in temperature.

It is safe to assume that all optical receivers have in their structure some errors present due to the degradation of optical signal during transmission and detection. The most common issue is the shot noise. A digital light wave can be characterized through bit error rate, which is customarily defined as the average probability of identifying a bit incorrectly. Some error-correction codes are proven helpful in improving the raw bit-error rate of an optical communication system. The photodetector in these receivers' circuits can use the common diode PN junction or a photo avalanche diode [2].

To date, WDM is the standard technology regarding optical networks., The end users only need to operate in the bit rate of the WDM channel in which can be chosen arbitrarily. As mentioned, the technique enables the use multiple wavelengths to send data over the same medium. It is an analog version of the FDM applied in optical systems.

The first WDM systems were those of low density. These were feasible to multiplex only a small number of optical channels. They increased their capacity present on the already installed fibers, through an optical channel of 1310 nm and other of 1550 nm. With the appearance of optical amplifiers with doped fibers, namely, Erbium-Doped Fiber Amplifiers (EDFA), Raman amplifiers , photodetectors optical filters, distributed feedback lasers, could enable the operation at different

transmission windows such as at 1550 nm (low losses) evolving this system into two technologies such CWDM and DWDM.

The transmission window at 1550 nm, corresponds to a specific minimal region of attenuation on silicon fibers. For monomodal silicon fibers, the attenuation is at the order of 0.2dB/km close to the final material limit constraint.

The DWDM system was developed and easily capable of reaching 40 Gbps while maintaining the QoS parameters. It differed mainly from CWDM on the aspect of how the channel is spaced along the spectrum, number of channels, and how the multiplexed signal is amplified. Importantly, the DWDM system according to the ITU-T recommendations are spaced at 0.8 nm or 0.4nm (for more than 1000 km). The normalized reference frequency from which the frequencies of the other channels are derived is 193.1 THz. Other recommendations include the spacing between several channels as for 12.5 GHz, 25 GHz, 50 GHz and 100 GHz [3]. From which one can use the following formula to form the completed DWDM fixed grid, and the flexible grid (6.25 GHz):

$$f_N = 193.1 + n \times \text{Channel Spacing Frequency} \quad [\text{THz}] \quad (2)$$

where n – is an integer (positive or negative including 0), f_N – allowed channel frequencies.

The capacity of transmission in embedded fiber is exponentially increased in this model. It carries the added advantage of not needing final equipment to be deployed. Thus, the DWDM lasers, transponders, amplifiers, multiplexers, filters can be placed between transmission mesh and over existing network architectures. This success is also relevant to the technology using the G.652 guideline from ITU, used on most optical systems [4][5].

On DWDM systems, the fluctuations of power per channel utilization need to be calculated. This is because since the EDFAs do not amplify evenly across the whole transmission spectrum. So, it is necessary to adopt gain flatteners to even out the amplification profile. This is similar to the case of Raman amplifiers laying the foundation of multifunctioning DWDM systems and affected current disciplines. As a result, adding or removing channels is rather challenging. Moreover, the optical amplifiers use the non-linearity present in the fibers, by interacting by itself those wavelengths. This allows the power to be transferred from one wavelength to another and from a pump laser at a given wavelength to a number of other wavelengths travelling through the same fiber. This induces nonlinearities in the process causing loss of signal (if propagated) [6].

In a more conservative pace, CWDM systems operate, due to wide channel spacing and a smaller number of channels. Devices with higher tolerances can be used leading to a significant reduction on equipment costs. The overall price of the solution on application in which the distance range does

not exceeding 120 km (MAN applications) or solutions in which saving costs are more important than transmission capacity. Depending on the project, these systems are better served with LWP fibers and their performance can be further increased by using linear optical amplifiers, contrary to DWDM only a few channels here are used varying from 4 to 16 in total.

The propagation of modulated light under high transmission rates on an optical fiber has been discussed in the literature. Most of the conducted studies and experiments use high density setups. It almost always results in the production of non-linear behaviour of the channel. These non-linearities that affect the signal during its propagation in the fiber are mainly related to a phenomenon originated by the Kerr Effect, which causes a variation in the refractive index of the medium as a function of the amplitude of the propagating carrier's electric field, resulting on transmission degradation, losses, dispersion [7].

3. Chapter II — Non-Linear Effects in DWDM

Transmitting beams with high modulation rate, where the length of large links implies the use of higher power input levels on lower systems the optical fibers, shows a behavior very close to linearity, different of when we submit it to more intense signals.

Thus, it can be noticed that the reference power even at the orders of milliwatts set of new co-prognostic frequencies within the original operating spectrum, can originate some disturbing effects on monomodal fibers with a core diameter. This occurs in general order of tenths of micrometers, due to their small diameter. A higher optical intensity related to an electric field in the fiber core is observed. Fields of those magnitude orders are most likely predisposed to induce nonlinear behavior on a fiber. On the other hand, systems that demand very high transmission rates are prompt to have small deviation of modulation pulses. This occurs in order to avoid time extensions that ultimately causes overlaps leading to increases in bit error rate.

In optics, the linearity is defined by the dependence or independence of the intensity phenomenon. Thus, non-linear effects are dependent on the intensities of transmitted waves. As in every nonlinear system, the output does not have a direct correlation with the input, so a superposition cannot be attained. There exist others non-linear effects that are related to the inelastic scattering like Stimulated Raman Scattering (SRS) and Stimulated Brillouin Scattering (SBS). In short, the light passes through a medium and part of this energy deviates the original propagation direction causing some light redistribution. If one considers the light energy as being the product of Photon Number and Photon Energy, it can be said that the scattering can also produce new light at frequencies different than the original light. This can occur due to inhomogeneous distribution of medium properties. The main difference between Brillouin and Raman scattering is the acoustic wave generated on Brillouin scattering the incident light as the density of the medium changes. Thus, the shift quantity of scattering light is equal to the phonon frequency. Raman scattering does not originate any waves and the scattering is attribute to the optical phonons [8].

For this work, the researcher solely focuses on the non-linearities that appear on DWDM systems like Self-Phase Modulation (SPM), Cross Phase Modulation (XPM), and Four-Wave Mixing (FWM), the last one being on primordial focus since the experiments here conducted where designed to evaluate such phenomenon.

3.1. Self-Phase Modulation

As already established, the power dependence in the context where optical powers lead to high optical intensities and on cases where high distance applications are used. The phase delay increases with the increase of optical intensities. The refractive index n of many optical materials has a weak dependence on optical intensity, I defined by [9]:

$$n = n_0 + n_2 \cdot I = n_0 + n_2 \frac{P}{A_{eff}} \quad (3)$$

Where n_0 is the ordinary refractive index of the material, P is the input power, A_{eff} is the effective area of the fiber core, and n_2 is the non-linear index coefficient (On silicon is approximately equal to $n_0 + 2.6 \times 10^{-8}\ \mu m^2 \cdot W^{-1}$). The non-linearity on the refraction index is known as the Kerr effect. The SPM appears when the Kerr effect appears on links with one unique wavelength. This causes optical power fluctuations of the light waves to be converted into phase fluctuations in the same wave, meaning the pulses will shift in different directions due to the phase shift fluctuations, broaden the spectrum of the pulse when associated with other linear effects (dispersion) [9].

The main parameter, γ, represents the magnitude of the non-linear SPM is defined by:

$$\gamma = \frac{c2\pi}{\lambda A_{eff}}, \quad (4)$$

Where γ is the nonlinear coefficient, λ is the wavelength, A_{eff} is the effective area of the fiber core, from this point the non-linear coefficient of the fiber is inversely proportional to the wavelength and the effective area of the fiber.

The SPM effect has two areas that can be of use, namely solitons and pulse compression. The soliton is a concept of a field that is self-balanced, where the properties of linear and non-linear fields are equivalent, here is the compensation of pulse broadening caused by dispersion using the SPM pulse result (compression) reaching a stable pulse propagating along the fiber.

3.2. Cross Phase Modulation

The XPM draw some similarity to SPM. However, it occurs due to channel interaction at the same medium, meaning that like on the SPM is caused by pulse power changes, power fluctuations in an adjacent channel A, while pulses are propagating simultaneously, results on phase modulation in an adjacent channel B. This can result in an asymmetrical spectral broadening and distortion of the pulse shape.

The changes of the refractive index can be described as[10]:

$$\Delta n^{(2)} = 2 n_2 I^{(1)} , \quad (5)$$

Where n_2 is the nonlinear index, the intensity $I^{(1)}$ of beam A causes refractive index change on beam B; The factor 2 is valid for beams that share the same polarization, for cross-polarized beams in isotropic media this value is replaced with $2/3$ [10]. As SPM the nonlinear effects are also dependent on the ratio of input optical power and the effective area (the cross-sectional area of the fiber), having the same delay mechanism (induced phase through Chirping and Dispersion), is important to mention that there is no spectral broadening in XPM or SPM without dispersion (chromatic) [1].

The XPM induced phase shift occurs when two pulses overlap in time, causing an intensity-dependent phase shift, and gives room to an enhanced temporal variation of instantaneous frequency (chirp), enhancing also the pulse broadening. At this point, one can say that the XPM is accompanied by SPM, limiting the light wave systems performance specially when the number of channels is large.

So instinctively, if the channels interact or overlap for a short time, and this can be done by increasing wavelength spacing, the resulting power fluctuations can be neglected. Further, due to fiber dispersion, the propagation constants of these channels change significantly that the corresponding individual channels walk away from each other, thus propagating from a few distance and are prevented from interacting further which leads to a reduction of the XPM effect [11].

Aside from pulses compression, that in general nonlinear systems are useful for, the XPM effect can be used in areas including frequency tunnelling and multiplexing, optical switching and wavelength conversion to state a few.

4. Chapter III — Four-Wave Mixing

The four-wave mixing process refers to third-order nonlinear phenomenon characterized by the appearance of a new fourth wave at a specific frequency when two or more waves are launched into the same fiber. This third originates from the nonlinear response of bounded electrons of the upper layer of the atoms of a material to an applied optical field, in which the polarization induced in the medium is non-linear. The process itself is very weak and required high intensity sources to generate it [12]. If we imagine a WDM, in which a set of coupled equations (Maxwell equations) are used to describe these low order nonlinear effects, meaning the nonlinear susceptibilities act as coupling coefficients between the waves of electromagnetism. Such electric field can be described as [11]:

$$E = \sum_{p=1}^{n} E_p \cos(w_p t - k_p z) , \tag{6}$$

And the relation of the nonlinear polarization is given by:

$$P_{nl} = \varepsilon_0 \chi^{(3)} E^3 , \tag{7}$$

Taking equation (5) into equation (6) and expanding the final expression, we get that the first term which is related to the SPM and XPM, while the subsequent terms (second, third and fourth) are not relevant due to phase mismatch (different signals travelling within the fiber at different group velocities) thus can be neglected. The last term of this expansion will represent the product of FWM [11].

$$\begin{aligned} P_{nl} = {} & \frac{3}{4}\varepsilon_0 \chi^{(3)} \sum_{p=1}^{n} E_p^2 + 2\sum_{q\neq p} E_p E_q E_p \cos(w_q t - t_p z) \\ & + \frac{1}{4}\varepsilon_0 \chi^{(3)} \sum_{p=1}^{n} E_p^3 + \cos(3w_q t - 3t_p z) \\ & + \frac{3}{4}\varepsilon_0 \chi^{(3)} \sum_{p=1}^{n} \sum_{q\neq p} E_p^2 E_q \cos\{(2w_p - w_q)t - (2k_p - k_q)z\} \\ & + \frac{3}{4}\varepsilon_0 \chi^{(3)} \sum_{p=1}^{n} \sum_{q\neq 1} E_p^2 E_q \cos\{(2w_p + w_q)t - (2k_p + k_q)z\} \\ & + \frac{6}{4}\varepsilon_0 \chi^{(3)} \sum_{p=1}^{n} \sum_{q>p} \sum_{r>q} E_p E_q E_r \cos\{(2w_p + w_q + w_r)t - (k_p + k_q + k_r)z\} \\ & + \cos\{(w_p + w_q + w_r)t - (k_p + k_q + k_r)z\} \\ & + \cos\{(w_p - w_q + w_r)t - (k_p - k_q + k_r)z\} \\ & + \cos\{(w_p - w_q - w_r)t - (k_p - k_q - k_r)z\} , \end{aligned} \tag{8}$$

These combinations ($w_p \pm w_q \pm w_r$) are the new frequencies generated by the new waves, paying attention to the ones that lay inside of the telecommunication band like for example combination ($w_p + w_q - w_r$ with $p, q \neq r$), if $p = q$ are identical, the FWM is considered degenerated.

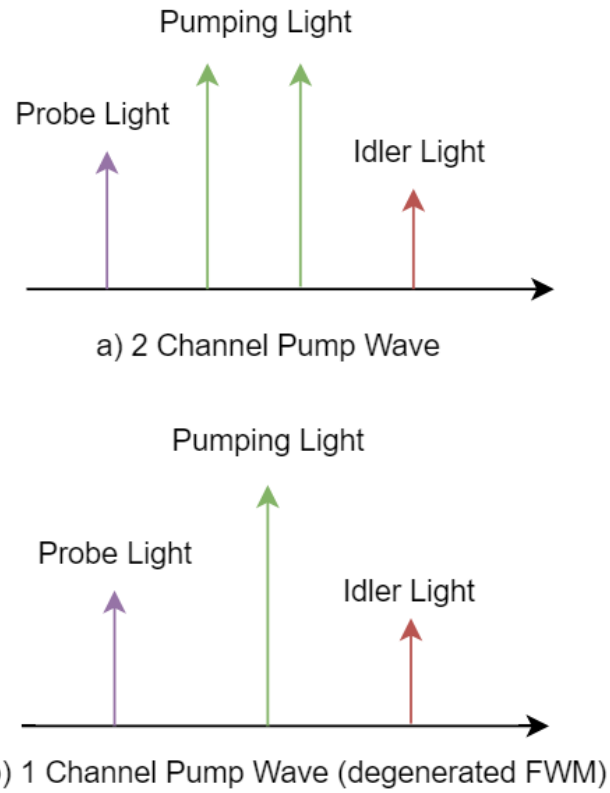

Figure 1 – FWM in the Frequency Domain | source: SemanticScholar [13]

The two frequencies p, q generate sidebands for both cases of the Fig. (1), the idler component will be the new generated component w_{pqr} and the probe light has the name suggests will be the frequency of the probe light w_r, if the number of wavelengths being launched to the fiber is increased from 2 to 3 the number of FWM products will grow exponentially from 2 to 9, this is established by the following formula [13]:

$$M = \frac{N^2}{2}(N - 1)\,, \tag{9}$$

Where N is the input signal number and M is the number of new generated components. There are certain factors that affects the efficiency of the FWM. If the dispersion and the channel spacing are considered the main requirements for this mixture to occur, and if the level of dispersion increases is hint that the FWM effect decreases since the signals will not be phased-matched long enough to

transfer sufficient power to the new components, meaning the group velocities between the signal waves and new generated waves will be mismatched summed with the increase of channel spacing will eventually lower the FWM effect, so a practical solution to mitigate this is to use Non Zero Dispersion Shifted Fibers (NZ-DSF).

Importantly, NZ-DSF fibers can reduce waveguide dispersion in single-mode fiber in the 1550-nm window (DWDM) by tailoring the refractive index profiles to compensate for the material dispersion, the result will be a large and negative waveguide dispersion.

However, the component-material dispersion is similar since those fibers are made with similar materials [15]. Another parameter that can be tweaked is the channel spacing. sending signals in the systems without uniform spacing, the generated wave components will not overlap the signal channels thus, these unwanted signal components can be easily filtered out.

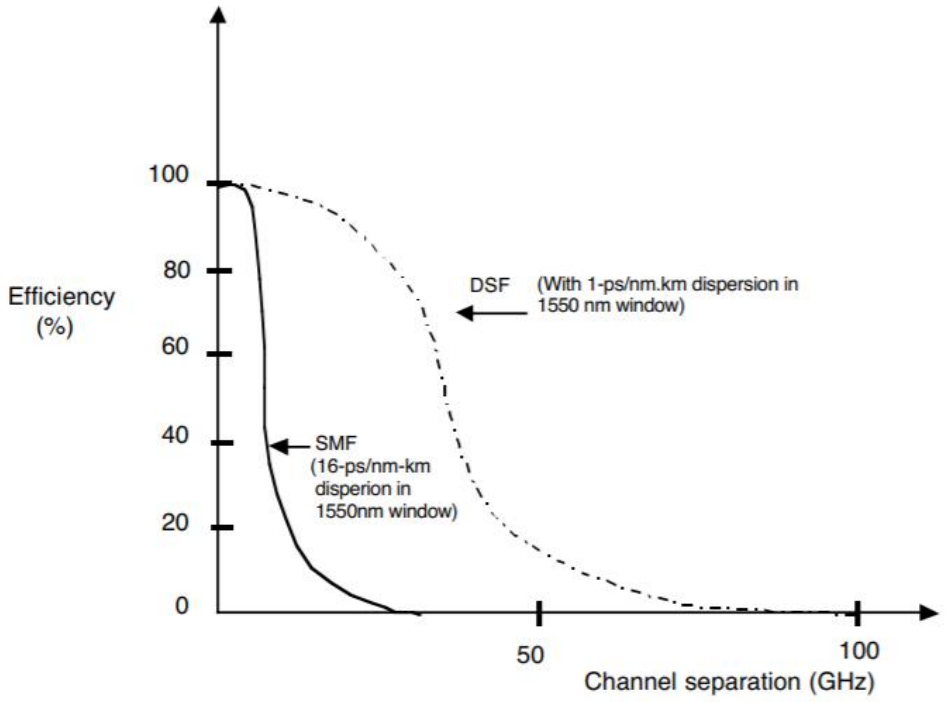

Figure 2 – FWM efficiency vs Channel separation | source: Jpier.org [11]

The curve in Fig. (2) shows that for conventional single-mode fibers (SMFs) the mixture is steady reaching close to 100% if the channel spacing is kept under 25GHz and for dispersion shift fibers (DSFs) these values are effectively mixed if the channel spacing is kept under 10GHz. The FWM, aside from its drawbacks, can be used to reduced quantum noise in a process called squeezing, and in wavelength conversions.

4.1. Methods used to avoid the creation of FWM

There is a set of techniques and rules that can be employed in ways that eliminate or prevent the appearance of this phenomenon. In the case of the use of a uniform spacing recommended by the ITU that uses a spacing of 100 GHz, 50 GHz, 25 GHz and 12.5 GHz for transmissions in DWDM, the increase in spacing between channels means that the new peaks they will be removed from the original signal and can be neglected or filtered out completely. Here there is a mismatch of the group velocities between the channels, reducing the number of channels that can be applied in the useful band of EDFA's. A reduction in the power released within the fiber, minimizes the effect of the FWM, which results in the use of line amplifiers in order to compensate for the attenuation of the optical link [12].

Another method that can be used and is also related to channel spacing is the use of uneven spacing, with this technique, the intermodulation products do not overlap with the useful information channels, in the case that the channels are evenly spaced, many FWM terms will agree with the useful information channels promoting the degradation of the signal to be discussed later.

Another technique that can be used has to do with a passive dispersion compensation that consists of inserting small strands of special fibers into the main link, generally this type of fibers has a dispersion value that compensates for the main fiber being used.

The use of fibers with a greater effective area such as NZ-DSF, which has relatively high dispersion values so as not to over-extend the pulse along the link and at the same time low enough so as not to reinforce the nonlinear effects varying its effective area between 55 to 100 micro square meters [14].

5. Chapter IV — Simulation Components

The Optsim™ is a state-of-the art software developed by Rsoft to design and simulate optical systems. This tool offers the flexibility of working over predefine simulation models or create our own model tailored to our needs. Its application range spans scenarios such as coherent optical communications systems, solitons transmission, DWDM/CWDM systems, different modulation formats scenarios and many others optical communications systems design, featuring different parameters and multiple engines.

This software at its version 5.2 will be at the base of the simulation. This help in the evaluation of optical parameters such bit error rate (BER), optical signal to noise ratio (OSNR), Q-Factor, and the eye diagram, all of it at the signal propagation level using a time domain using split step Fourier method (SSFM) to solve the complex differential nonlinear Schrodinger equation (NLSE) which takes into account linear and nonlinear effects and their influence to optical signal distortions[16].

The SSFM can be obtained by using a time-domain split step (TDSS) algorithm or a frequency domain split step (FDSS). Between them, FDSS is easier to implement. However, it is more likely to throw some calculation errors [16], therefore our simulator uses a TDSS engine using FIR filters, to calculate the nonlinear effects, which draws more computational resources but proven more reliable.

Considering the NLSE, describing the optical signal propagation over the fiber, can be described by equation (10) [16]:

$$\frac{\partial}{\partial z} \cdot A(t,z) = \left(\widehat{D} + \widehat{N}\right) \cdot A(t,z)\ , \qquad (10)$$

Where z is the length of the fiber, $A(t,z)$ is the complex optical field, $\widehat{D}$ is the linear effects operators (dispersion, attenuation) and $\widehat{N}$ is the nonlinear effects operators (FWM, XPM, SPM and others).

The operator $\widehat{D}$ can be replaced, by its impulse response on the discrete time domain, so is mathematically correct to calculate its influence on the complex optical field using product convolution, translating this into TDSS terms we obtain equation (10) [16]. There some time delays between different wavelengths can be seen.

$$A_L[n] = A[n] * h[n] = \sum_{k=-\infty}^{\infty} A[k] \cdot h[n-k], \qquad (11)$$

5.1. Eye Diagram

The eye diagram is a useful tool to study the effects of interference between symbols and damage in the transmission channel. It provides information related to the amplitude noise and the time jitter, while both are combined when we use the BER indicator. It is also described as eye pattern is a strong indicator of the quality of the signal at the receiver side. An oscilloscope is connected to the receiving end of link, in which the overlapping sweeps of different segments of a long data streams at a rate of one- or two-bit periods are exhibit, meaning the signal at the receiver is continuously overlapped by a pseudo-random signal synchronized at the master clock. These many transitions after overlaying causes positive and negative pulses to superimposed on each other, resulting in a picture resembling the opening of an eye [17].

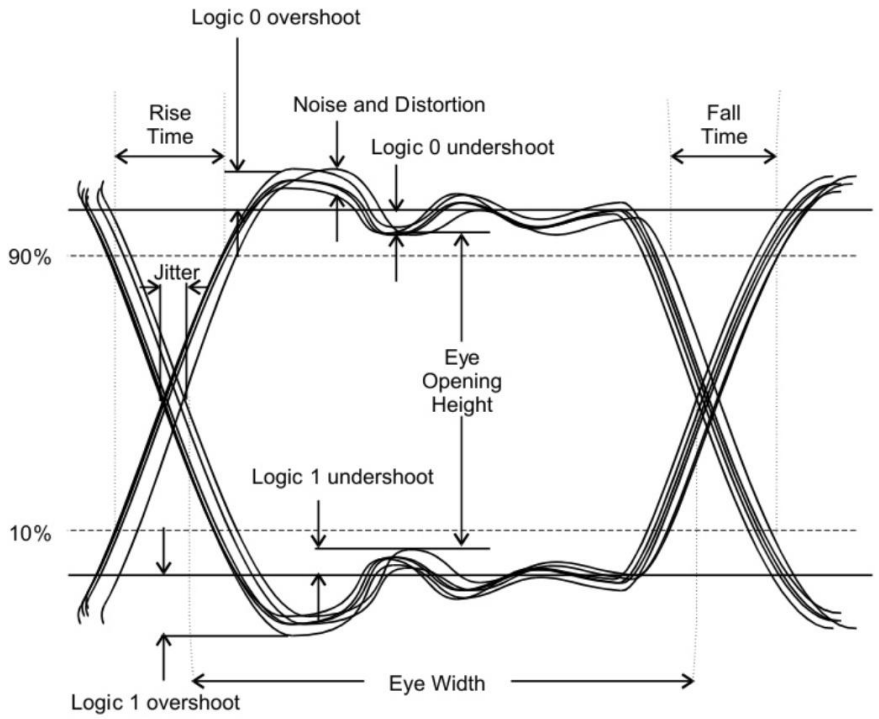

Figure 3 – Eye Diagram | source: IDC Technologies © 1991 – 2020

Measurements can be obtained by properly analysing the diagram at Fig. (3) such as noise, jitter, pulse quality, rise and fall time, overshoot, undershoot, period, settling time and others.

The widest opening of the eye is considered the best time interval in which the receiving signal without pulse interference from adjacent channels can be sampled. Similarly, the height of the largest

opening is the best time to sample the received waveform. The height reduces its size when exposed to the amplitude distortion of the data signal.

5.2. OSNR, BER and Q-Factor

The OSNR is defined as the ratio of the signal power to noise in an optical channel. This key parameter is important to estimate the performance of the optical networks, since it also suggests the level of impairments when dealing with optical systems that include amplifiers, since the OSNR decreases with the amplification stage limiting the number of optical amplifiers while designing an optical network, in particular, DWDM systems need to surpass their OSNR limit to ensure error free operation [18].

$$\mathrm{OSNR} = 10\log_{10}(P_S/P_N), \tag{12}$$

The OSNR indirectly reflects BER, that is given by the ratio of total incorrect received bits to the total amount of transmitted bits, for this to be calculated the optical signal is converted to electrical signal, a lower the value of BER the better the system is performing. In high-speed optical data communications, the required BER ranges between 10^{-9} to 10^{-15} unitless, a common value being 10^{-12} unitless [19].

Another way of calculating the BER and OSNR is to use the Q-Factor Parameter. The Q-Factor is a quality system parameter that matches a required OSNR to a BER value, having a one-to-one relation to BER.

$$\mathrm{BER} = \frac{1}{2}\,\mathrm{erfc}\left(\frac{Q}{\sqrt{2}}\right), \tag{13}$$

Without a measure of symbols interference and assuming gaussian distribution of the pulses the Q-Factor can be calculated using the logic values of overshoot and undershoot just like in formula (12).

$$Q = \frac{|\,\mu_1 - \mu_0\,|}{\sigma_1 + \sigma_0}, \tag{14}$$

Where μ_1, μ_0 are the mean values at different logical levels and σ_1 , σ_0 the standard deviation at different levels, of the received signal.

6. Chapter V — Simulation Experiments

6.1. Simulation Experiment: FWM necessary appearance conditions

The first experiment will consist of 2 channel systems, both using a setup with a pumping laser, spacing of 0.50 between them and both equal in configuration with a 15 dBm input power. They are interchanging frequencies between 192.515 and 193.765 THz, and further parametrize into frequencies 193.125 and 193.175 respectively spanning a Source/Destination path of 100 Km. The fiber used has a 62/5 core effective area with a polarization mode of 0.1 and 0.2 dB/Km in fixed loss value (attenuation). The goal of this first experiment is to observe extra components in our output, which was achieved by setting close spacing channels and small dispersion as referenced in Chapter III. This experiment serves to verify the necessary conditions for the achievement of crosstalk's on the output spectrum.

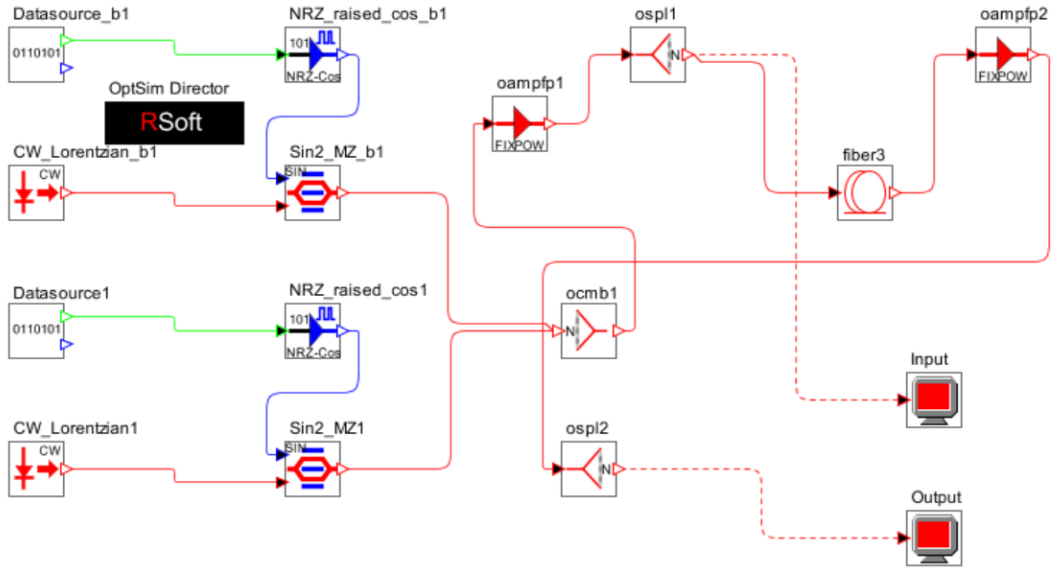

Figure 4 – Degenerated FWM [Reference Optsim Manual]

Both data sources (DataSource_b1 & Datasource1) have the same 10 Gbit/s rate generating a total of 31 Gbit/s and is encoded by the NRZ raised cosine block. The small amount of power generated by both sources is amplified using topology applications, to provide the power necessary to feed the network. The chosen amplifier (oampfp1) has a flat gain and in best-case scenarios it can gain 1db. The amplified signal is then feed to an optical splitter (ospl1) where the first measurement (the input signal) is established, which can be reviewed in Fig. (5).

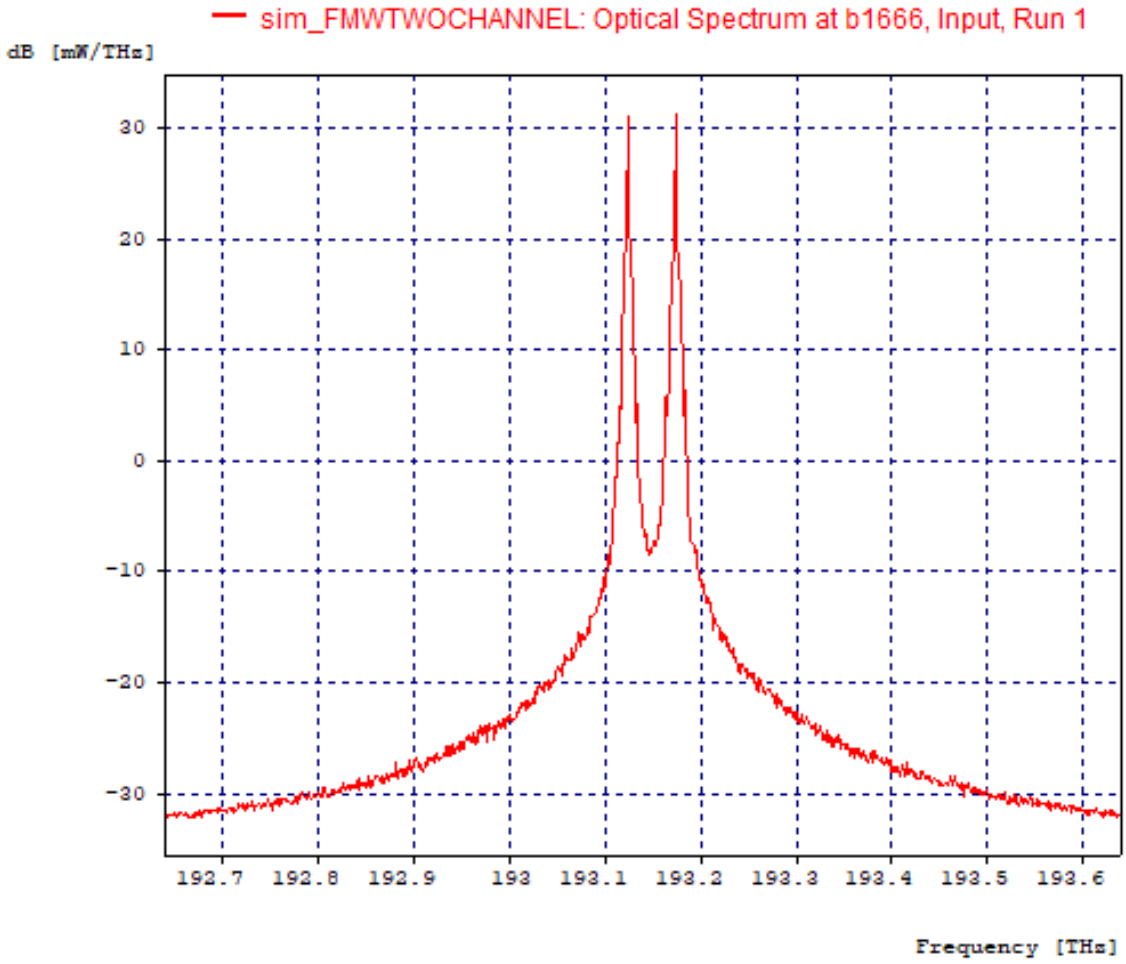

Figure 5 – Input Signal

The original setup gives a clear visualization of the 2 pumps, and their epicenter marks the respective frequencies. The expected output should give us 2 new frequency components after traveling further. Fig. (5) depicts a high output power, with narrow channel spacing between central frequencies, and the attenuation is near zero ($0.2\ ps/nm/km$).

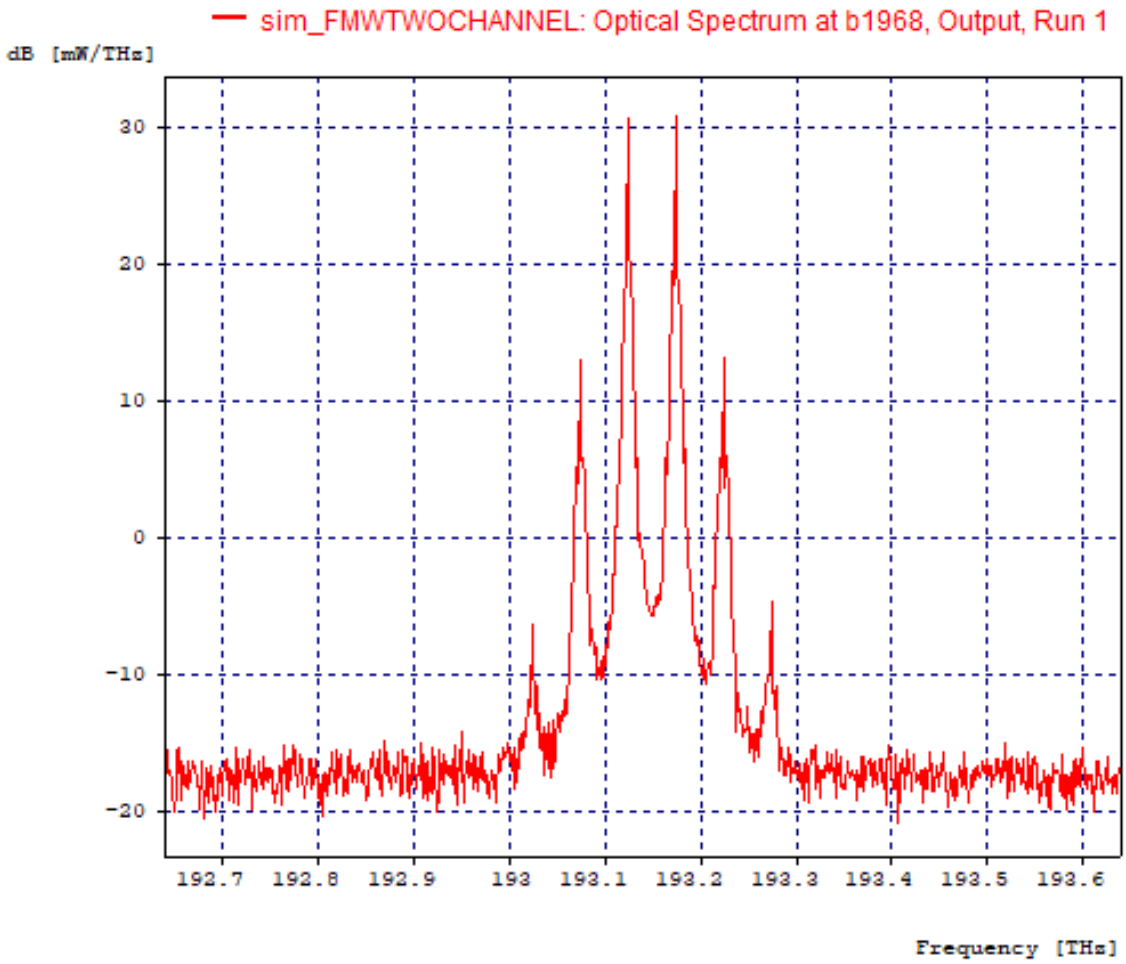

Figure 6 – Output FWM Result

The new frequency components observed are located at 193.075 and 193.225 THz respectively. Fig. (6) was modified using a Lorentzian filter, where a smoother curve is observed, Fig. (7). The other results below 0 can easily be filtered.

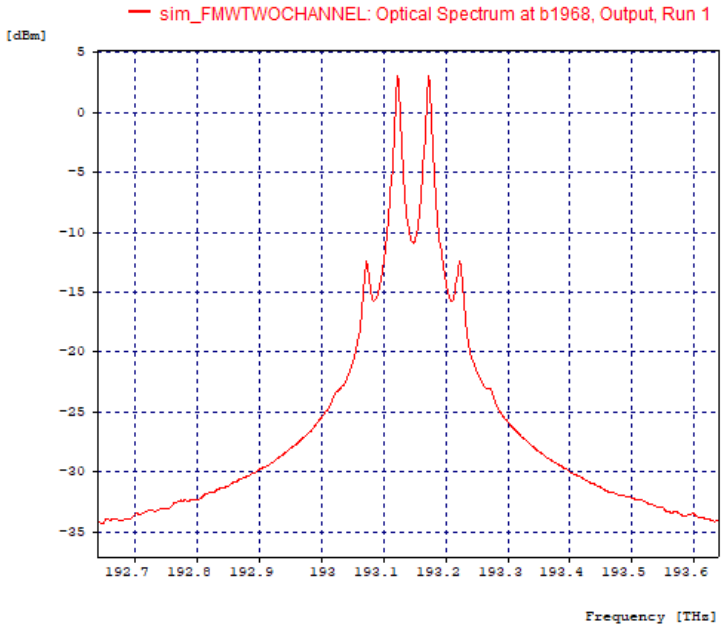

Figure 7 – Output Smoother FWM effect

As shown above, the FWM is a construct of high power at the input, with dense channel spacing and near zero dispersion fiber. Thus, meeting one of this 3 requirements can easily mitigate any type of issues. By increasing the dispersion levels at the optical fiber from 0.2 to 0.8 ps/nm/km, it is visible that the new peak components have decreased.

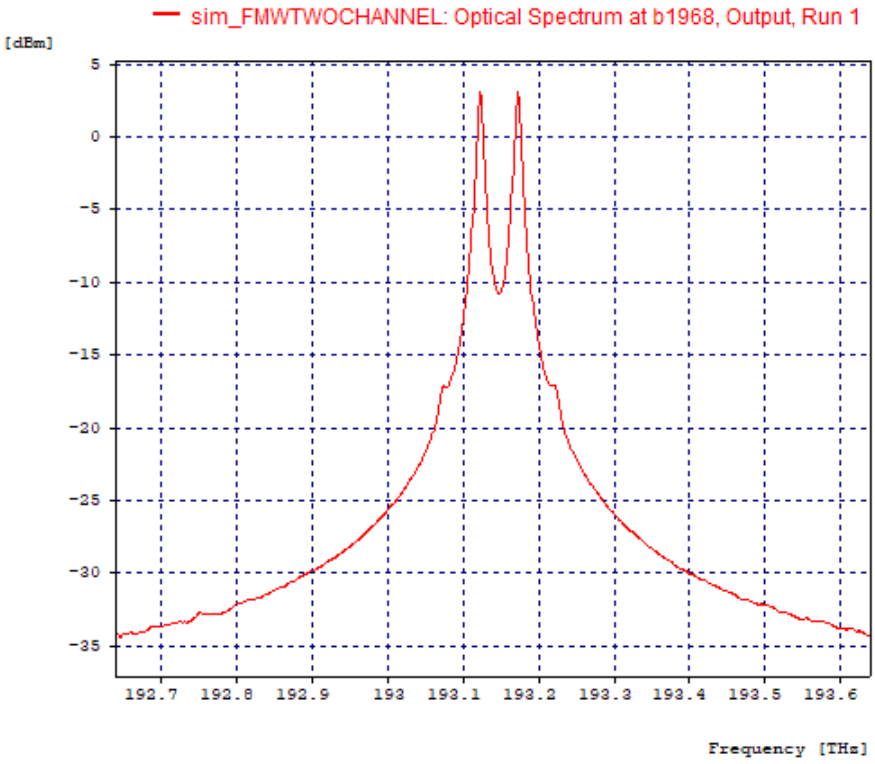

Figure 8 – FWM output with increased Dispersion

It's clear that dispersion plays a role on the appearance of extra components, as demonstrated on both Fig. (7) and Fig. (8). Another parameter that contributes for the appearance of extra frequency components is the high power on the input, by resetting our initial value of dispersion and reducing the input power by $1/1000$ and reducing the gain of the amplifier. This will result on the disappearance of extra components, since the amplification gain is flat no variation in the output should be observed, resulting in a suppressed FWM.

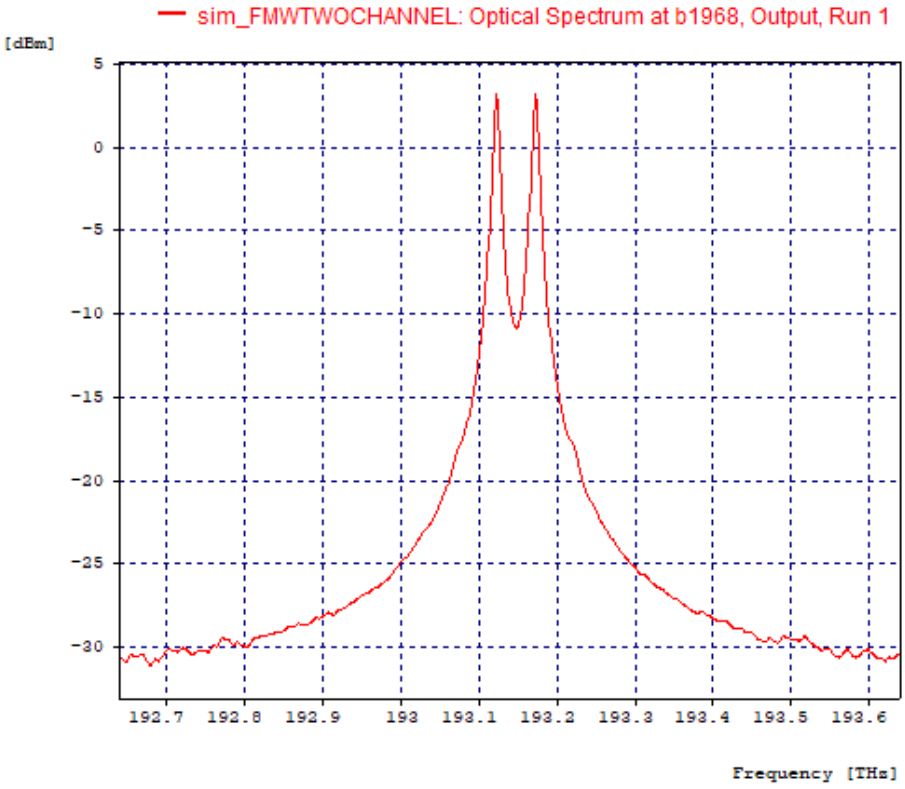

Figure 9 – FWM Output with Decreased Input Power

The final requirement is related to the channel spacing, so once again the simulation will be reset and the channel spacing will be extrapolated beyond the DWDM constraints (more than 1 nm). The target frequencies will be 193.125 and 193.275.

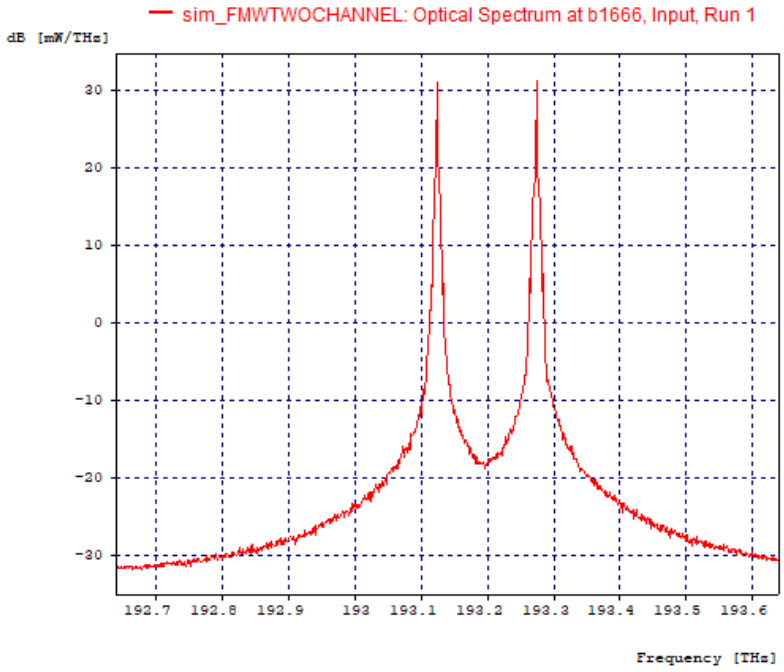

Figure 10 – Input Signal with Increased Channel Spacing

The corresponding output will be render inefficient due to a steep decrease in peak power, rendering the FWM inefficient.

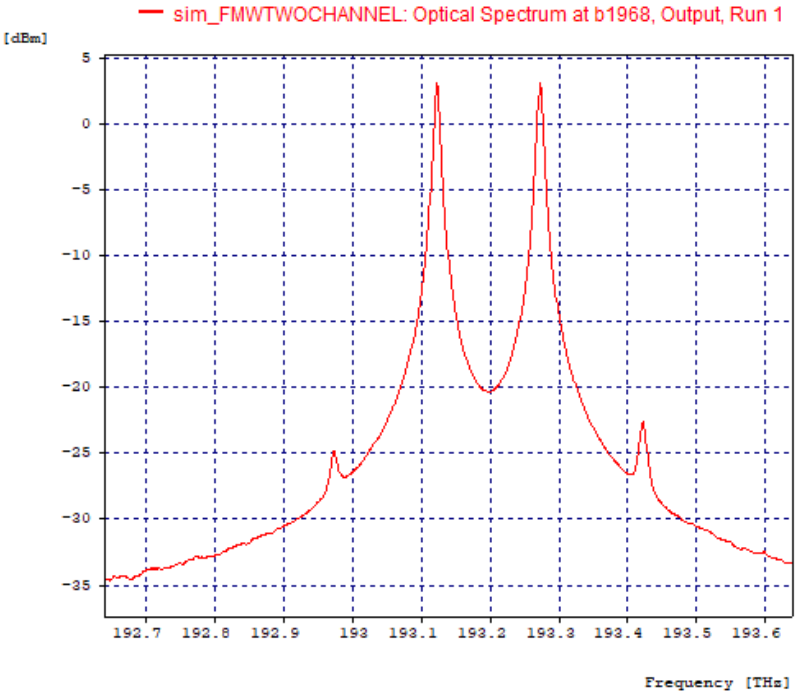

Figure 11 – Output Signal with Increased Channel Spacing

6.2. Simulation Experiment: FWM performance vs necessary appearing conditions

The main goal of this second experiment is to observe the performance of a system under the FWM effect. For this setup the main indicators will be the eye diagram paired with Q-Factor and BER. The experiment consists of a 4 Channel WDM Transmitter with a channel spacing of 100 GHz, and 10 Gbit/s rate that is fed to a 10 dB fixed gain amplifier. The distance between the Source/Destination is the same as in the first experiment.

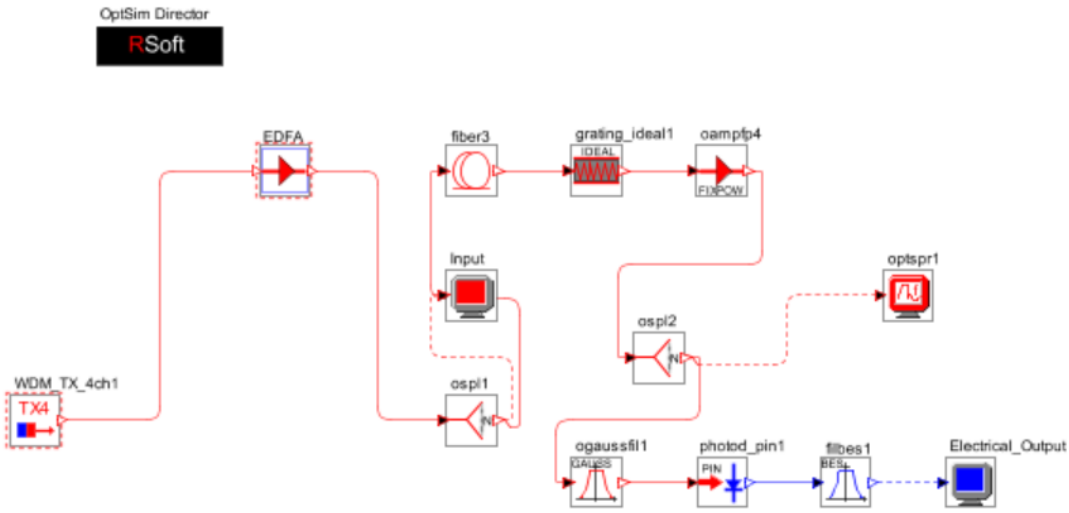

Figure 12 – Non-Degenerated FWM

For this experiment the used fiber will have 0 ps/nm/km dispersion at first, and the power of the WDM transmitter will change prompting us to do a parametric comparison among all the described performance indicators. Specifically, the goal is to analyze how these parameters of signal quality are related to the existing preconditions of the appearing of FWM. The second part of the experiment will consist of a fixed reference power level at the input and the dispersion values will change in order to establish a key relation among the indicator parameters.

6.3. Input Power Dependency on system performance

As described our metrics table of varying input power will range from 10 to -10 dBm and the relevant values of the performance indicator will be collected.

Table 1 – Measured Power Levels

Input Power[dBm]	Q-Factor max [-]	Q max[dB]	Q-Factor [-]	Q-Factor [dB]	BER [-]
1.00E+01	3.60E-01	-8.84E+00	truncated	truncated	truncated
8.00E+00	3.30E-01	-9.52E+00	truncated	truncated	truncated
6.00E+00	3.10E-01	-1.02E+01	truncated	truncated	truncated
4.00E+00	3.40E-01	-9.47E+00	truncated	truncated	truncated
2.00E+00	3.30E-01	-9.72E+00	2.63E+00	8.41E+00	4.00E-03
0.00E+00	3.10E-01	-1.01E+01	2.75E+00	8.80E+00	2.93E-03
-2.00E+00	2.70E-01	-1.12E+01	3.16E+00	9.99E+00	8.66E-04
-4.00E+00	2.40E-01	-1.23E+01	4.57E+00	1.32E+01	2.46E-06
-6.00E+00	2.30E-01	-1.29E+01	7.32E+00	1.73E+01	5.26E-13
-8.00E+00	2.30E-01	-1.28E+01	1.10E+01	2.08E+01	3.17E-28
-1.00E+01	2.30E-01	-1.26E+01	1.38E+01	2.28E+01	1.00E-40

From power level 10 dBm till 4 dBm power level, the values for Q-Factor and BER had deteriorated to the point that the sensitivity scale of our measurement devices truncated the values to be standard ate BER 0.0227501 and Q value [dB] = 6.02060 and Q value [-] = 2.00000. This is a strong indicator of the poor quality of the output signal. The resulting output spectrum from Fig. (10) till Fig. (13), show that FWM products blend with the actual signal.

Without the option of doing any post processing by lowering the input signal, the difference between useful signal and crosstalk's is visible. These values of input power are related to the input laser. However, the input channel power is in the order of 10dBm + the input power laser, after the amplification stage this power is feed to the actual fiber when the FWM is originated. In real life scenarios lasers are used from values bellow 0 dBm and the actual parameters of the network also influence the BER.

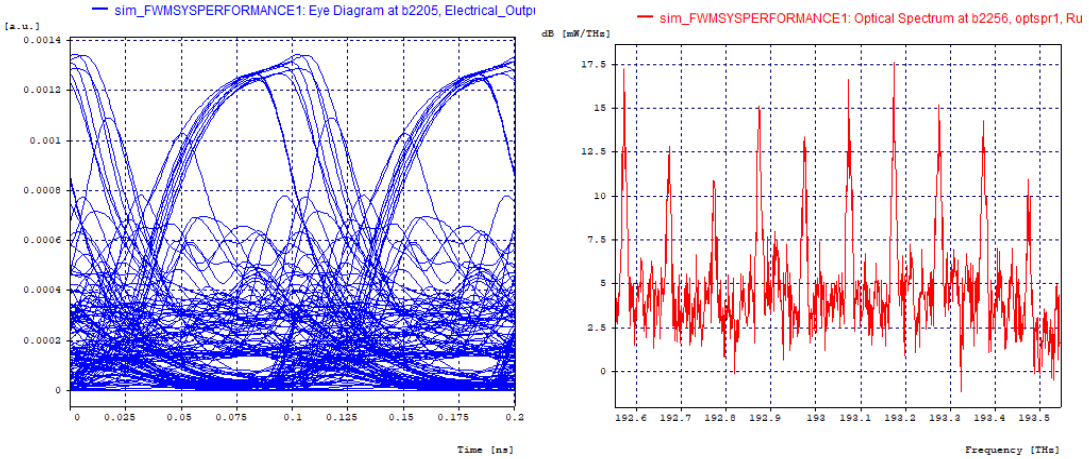

Figure 13 – FWM Eye Diagram & Output Spectrum at 10 dBm Power and 0 ps/nm/km Dispersion

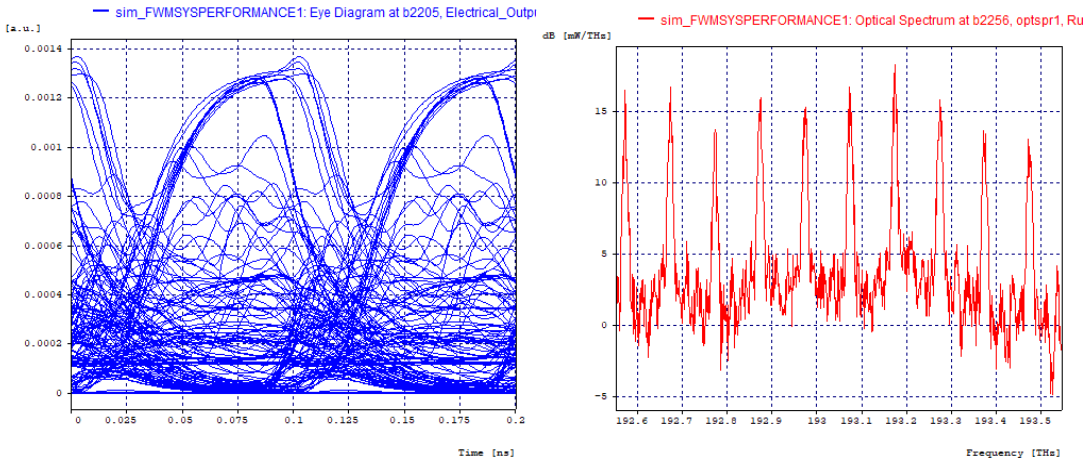

Figure 14 – FWM Eye Diagram & Output Spectrum at 8 dBm Power and 0 ps/nm/km Dispersion

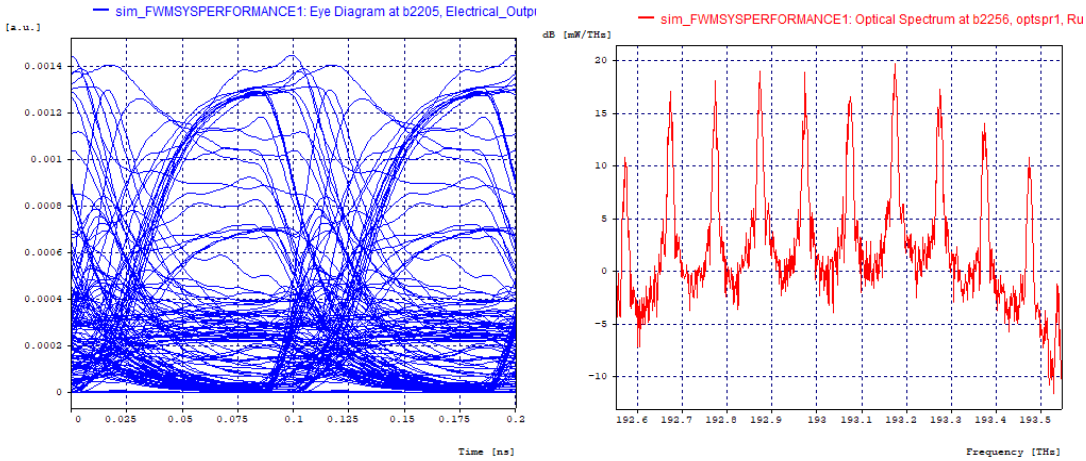

Figure 15 – FWM Eye Diagram & Output Spectrum at 6 dBm Power and 0 ps/nm/km Dispersion

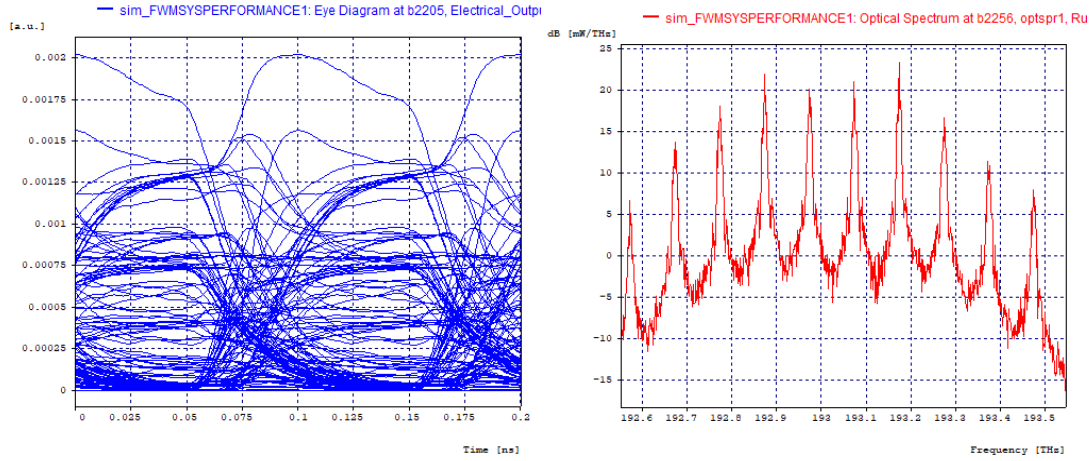

Figure 16 ─ FWM Eye Diagram & Output Spectrum at 4 dBm Power and 0 ps/nm/km Dispersion

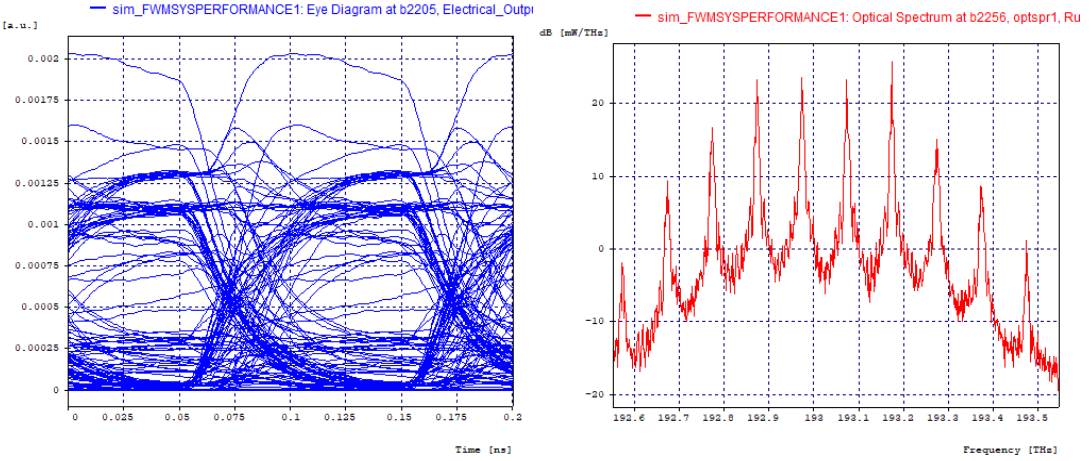

Figure 17 – FWM Eye Diagram & Output Spectrum at 2 dBm Power and 0 ps/nm/km Dispersion

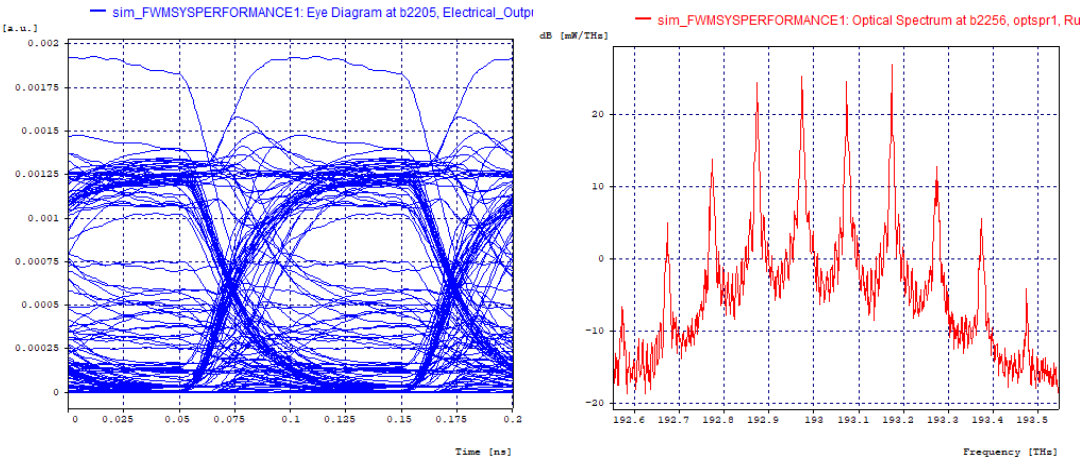

Figure 18 – FWM Eye Diagram & Output Spectrum at 0 dBm Power and 0 ps/nm/km Dispersion

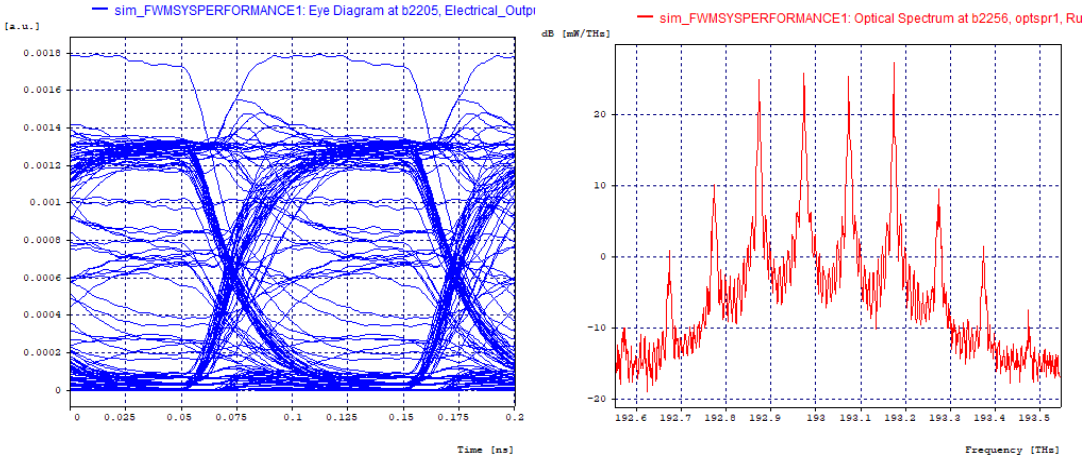

Figure 19 – FWM Eye Diagram & Output Spectrum at -2 dBm Power and 0 ps/nm/km Dispersion

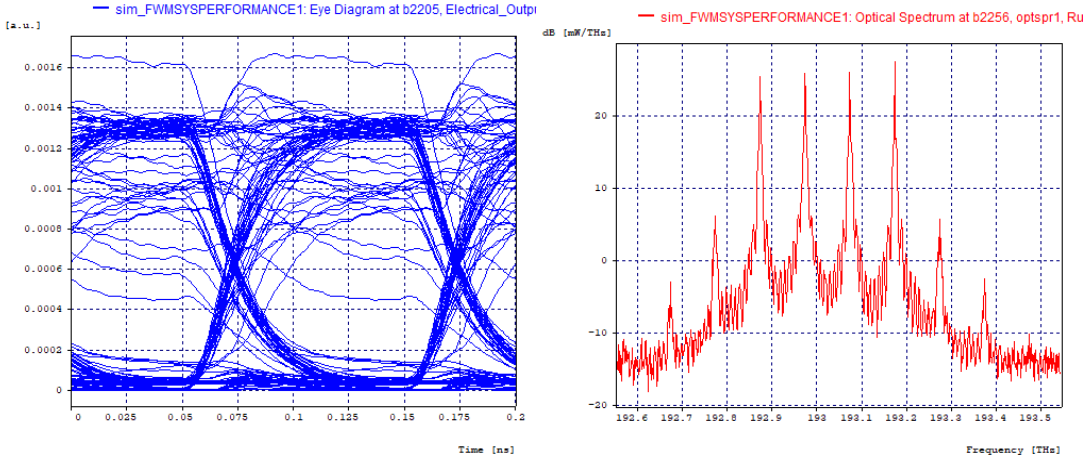

Figure 20 – FWM Eye Diagram & Output Spectrum at -4 dBm Power and 0 ps/nm/km Dispersion

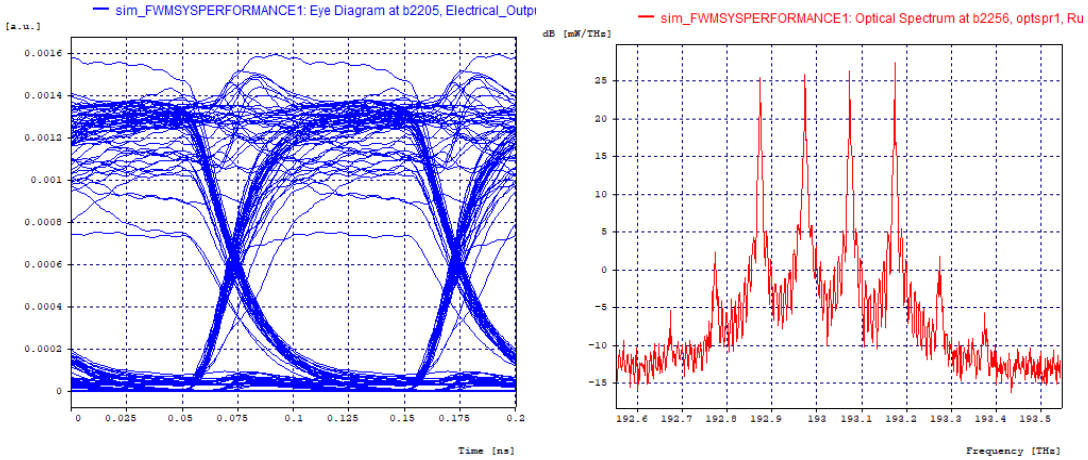

Figure 21 – FWM Eye Diagram & Output Spectrum at -6 dBm Power and 0 ps/nm/km Dispersion

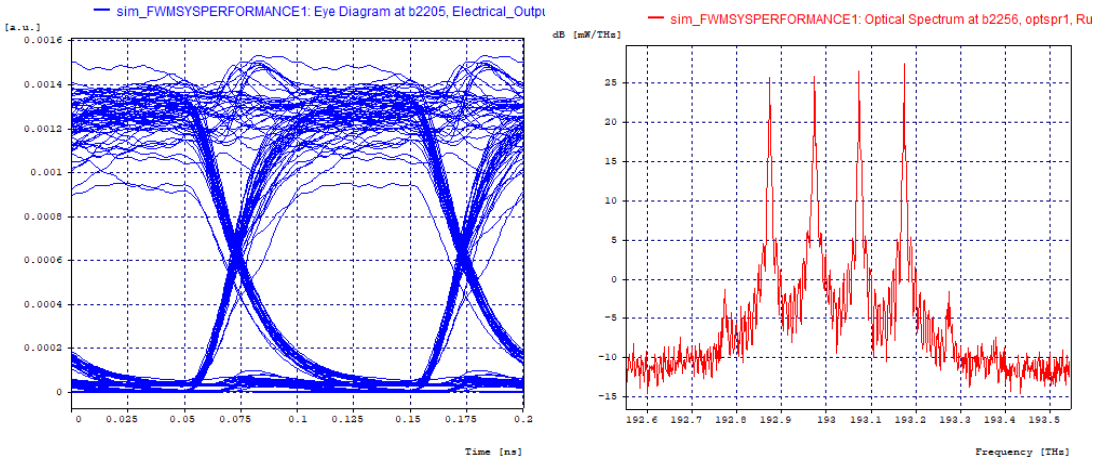

Figure 22 – FWM Eye Diagram & Output Spectrum at -8 dBm Power and 0 ps/nm/km Dispersion

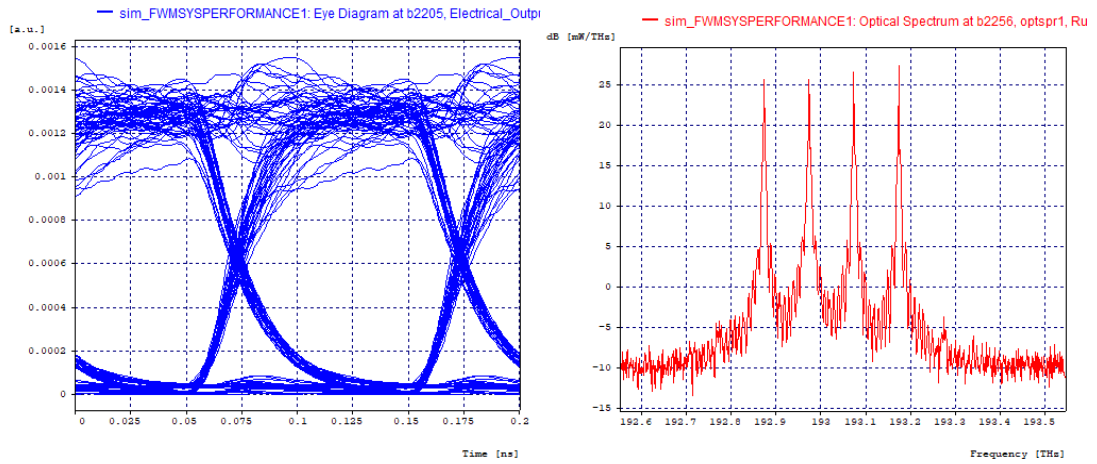

Figure 23 – FWM Eye Diagram & Output Spectrum at -10 dBm Power and 0 ps/nm/km Dispersion

Let's consider a more definite approach and measured the actual power going in the fiber and the output power of the network. Following the original chart from the Table 1. where the input power is referenced in a pre-amplified stage.

Table 2 – Input Channel Power Vs Quality Parameters

Input Power [dBm]	BER [-]	Q-Factor[dB]
12.29	4.00E-03	8.481453
10.29	2.95E-03	8.736475
8.29	8.72E-04	9.931815
6.29	2.31E-06	13.163228
4.29	4.02E-13	17.299362
2.29	3.22E-28	20.802906
0.29	1.00E-40	22.890967

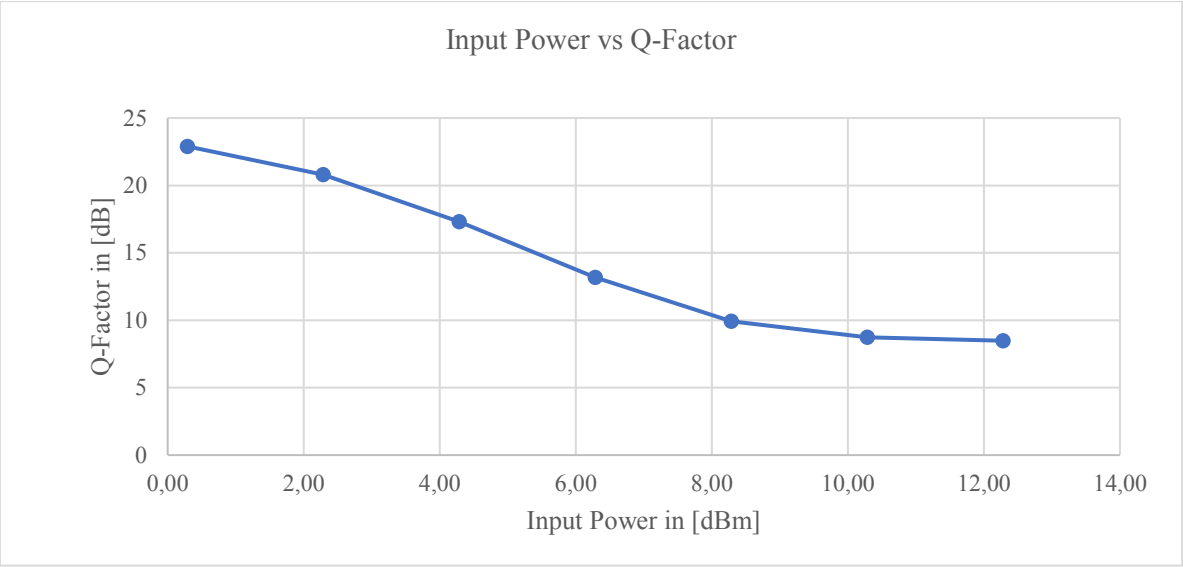

Figure 24 – Input Power vs Q-Factor

Figure 25 – Input Power vs BER

The 2 curves on Fig. (24) and (25) show that if the power level increased the Q-Factor will simultaneously decrease as the BER increases. There is an approximation on Fig.(25) that smooths the curve between the points 4 and 6, altering the original results, in reality there exists a steep drop between these 2 points.

For this short haul system, the advisable is to have less than 4.29 dBm in the channel fiber to assure smooth operation. The shape of the eye displayed among Fig.(17-19) suggests that the amplitude peaks noise and the signal delay in the system is high. More comprehensible than the BER as the 2 contributors are separated, so the attenuation and dispersion values influence the shape of the eye. At Input Channel power of 0.29 dBm is observed the best transmission.

6.4. Dispersion Dependency on system performance

As mentioned, it is important to see the impact of the dispersion for a link. In this scenario the referenced input power channel will be fixed at 10.29 dBm and different values of dispersion were swapped during the simulations.

Table 3 – Dispersion Parametric Run

Dispersion [ps/nm/km]	BER [-]	Q-Factor[dB]
0.00	2.95E-03	8.736475
0.10	3.69E-03	8.587611
0.20	1.74E-08	14.878895
0.30	1.52E-17	18.494450
0.40	7.94E-26	20.643651
0.50	2.51E-39	22.451850
1.00	1.00E-40	23.713541
2.00	1.00E-40	23.664683
3.00	5.55E-33	21.545083
4.00	5.89E-24	20.210243
5.00	4.24E-16	18.341720

By comparing both Fig. (18) and Fig. (26), some crosstalk on the network were suppressed and the transmission was improved in an exponential way as Table 3 suggests. However, the FWM products are still there. The values for dispersion ranging from 0 till 0.50 ps/nm/km are improving BER and Q-Factor by effectively reducing the FWM crosstalk's present in the signal. With Fig. (26), the shape of the eye diagram remains oval, clearly showing a better signal to noise ratio when compared to Fig. (27). The values ranging from 1 till 5 ps/nm/km are destroying signal performance, but no FWM product is observed or at least is not noticeable as shown in the spectrum at Fig. (27). For dispersion values it is important to carefully adjust the ratio between accounting for Cross Talks and System performance. The phase matching is finite, so larger values of dispersion limits the FWM effect.

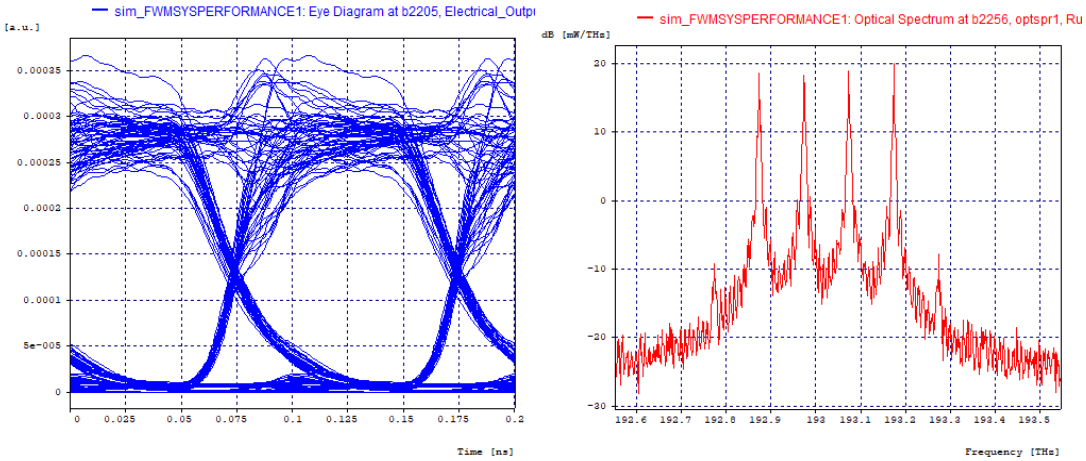

Figure 26 – FWM Eye Diagram & Output Spectrum at Reference Power and 0.5 ps/nm/km Dispersion

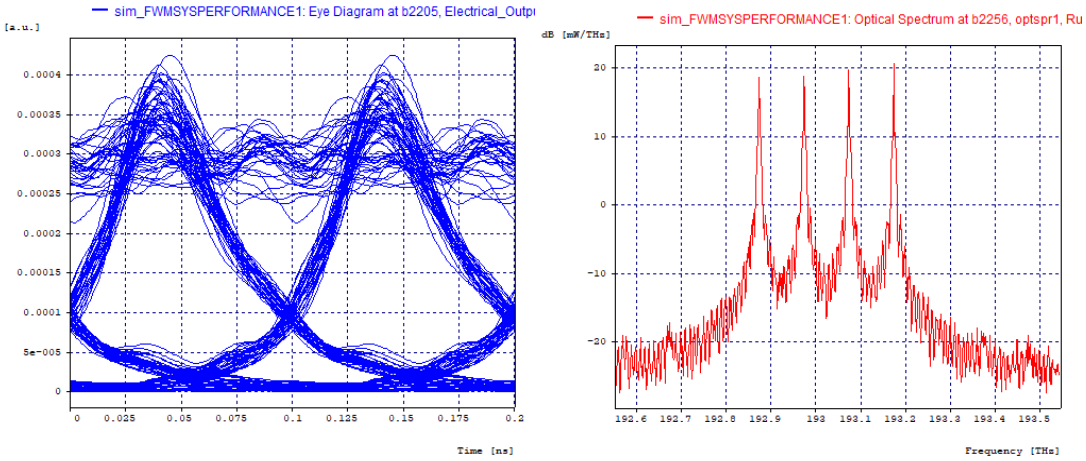

Figure 27 – FWM Eye Diagram & Output Spectrum at Reference Power and 5 ps/nm/km Dispersion

6.5. Channel Spacing Dependency on System Performance

Narrow margins used in channel spacing presents the opportunity of transmitting larger channel in the same bandwidth. Experiment 1 produced results that suggested that while increasing channel spacing the FWM products will dissipate in the spectrum, so the expectation is that for an increase of channel spacing a smaller BER and larger Q-Factor. In this scenario the reference power is at 10.29 dBm and the reference dispersion 2 ps/nm/km. The crosstalk is present on this network.

Table 4 – Channel Spacing Parametrization

Channel Spacing [GHz]	Q-Factor[dB]	BER [-]
100.00	23.664683	1.00E-40
75.00	21.889730	1.25E-33
50.00	12.133464	3.31E-05
40.00	7.6114900	8.10E-03

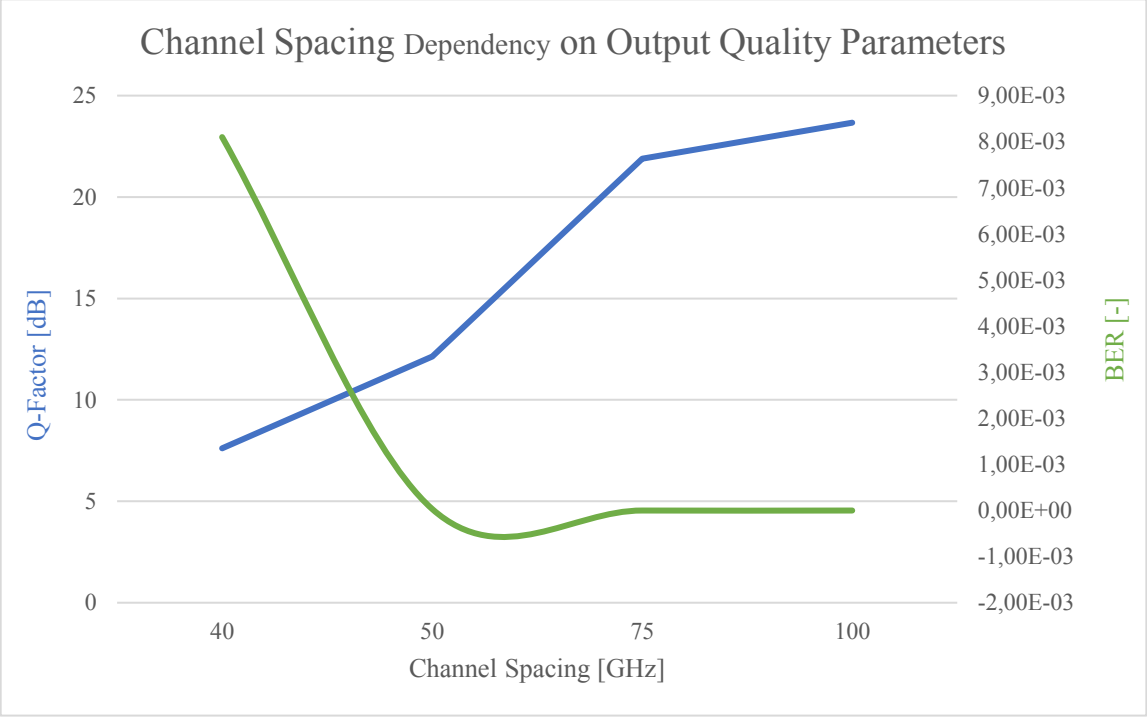

Figure 28 – Channel Spacing vs Quality Parameters

From the data collected is clear that higher channel spacing values need to be accomplished to achieve a better system performance, as the initial assumption suggests, however these values do not

progress continuously since, there exists only a determine number of recommended channels spacing.

7. Chapter VI — Practical Experiments

This chapter is based on a practical laboratory experiment in which by considering the concepts described and simulated on previous chapters the appearance of FWM was observed. For this experiment the following materials were used: an EXFO OTDR FTB-500, a Thorlabs S7FC1013S Semiconductor Optical Amplifier, an EXFO FLS-2600B tunable laser source, and 2 Small Form-Factor Pluggable(SFP) modules mounted on a HP V1910-16G Switch, and a NZDF (non-zero dispersion fiber) spanning 50 Km, and a 3X1 MUX, LC/PC patches and SC/PC patches.

Figure 29 – Illustration of the Components used at experimental laboratory | source: [20][21][22][23]

During this generating process it was establish that the DFB laser generated by the tunable laser source should be located in between the 2 SPF DWDM transceivers signal since they have fixed wavelengths it simplifies the work of fitting a third signal to interact in their close spacing in order to create some cross talks fulfilling the condition of dense channel spacing, these lasers are in the Continuous Wave (CW) regime and are placed in the transmitter being multiplexed with the DFB laser. This is relevant from the non-degenerated FWM system. The generated setup will include one SPF module and the tunable laser source.

Another important criterion that needs to be considered while selecting these wavelengths is the effectiveness of the DWDM systems, DWDM system are effective between the C band (1525-1565 nm) and L Band (1570 nm – 1610 nm). The transmission windows have different gains establish depending on which wavelength is used to transmit it automatically determines the choice of our amplification stage gain. When compared the SOA as higher noise than EDFA, this amplifier as an output saturation power set not higher than 6.8 dBm, this associated with their quick ignition response and non-linear effects makes it difficult to use as an inline amplifier, but for this particular setup the

gain is not linear, this conclusion was reached after varying the pump of the amplifier EDFA and registering the output power of our distinct laser sources as described in the upcoming tables.

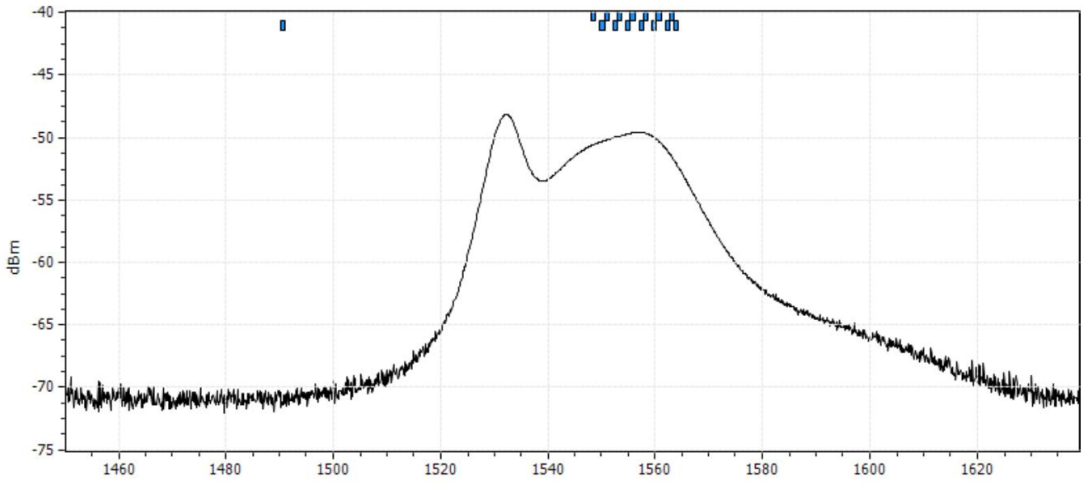

Figure 30 – EDFA Gain

For a weak peak pump we see, at beginning the response is weak, but if we increase, we will enter the linear regime where it increases rapidly, all the way to the maximum value at 156mA reaching saturation. The level in noise is at the level of 65 dBm, some connectors create a better match than other connectors. This gain curve was registered at the maximum pump current for this module was set at 156 mA, and depending on the temperature set on the SOA, the lower the temperature higher the gain, the final optimal combine gain was 52.3 dB.

This concludes the first setup of our experiment in which was simplified into the following:

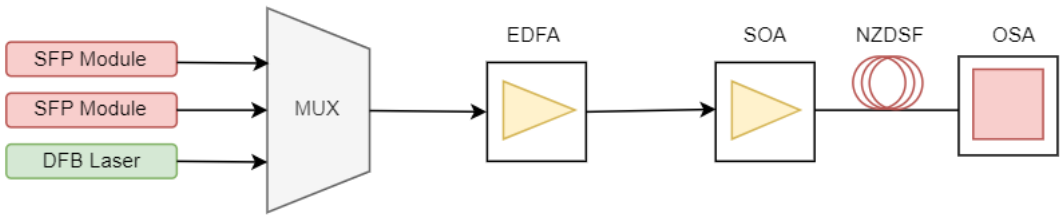

Figure 31 – Experiment Schematic

The most relevant part on this setup is the amount of power entering the fiber as mentioned large power at the input of a fiber with zero or close to zero dispersion generates non-linear effects, so the section between the final amplification stage and the input of the fiber needs to be investigated. The OTDR FTB-500 by EXFO was the equipment used to verify the spectrums represented on this chapter.

Table 5 – Initial Input Values Entering the fiber

Laser Sources [nm]	Power in [dBm]
1531.880	-21.74
1532.350	-17.62
1532.670	-21.63

These values per say are not sufficiently large enough to generate crosstalk's or sideband peaks, also we should not have such a huge drop when compared to the initial 0 dB, so the next logical step was to rearrange the connectors to first discard equipment malfunctioning and to baseline the measurement. The losses on optical connectors and patches are mostly due to inappropriate handling, impurities and patching adaptors, these group of losses are of an extrinsic nature, in order to suppress them is necessary to properly clean the tips of the connecters with isopropyl alcohol and some cleaning tissues, to not bend the patches into a right angle, nor using cables with different properties, and good connectors (they were not design to be disconnected several times).

After the audit, and ensuring the proper cleanness of the connectors the results were:

Table 6 – Input Values Entering the fiber after the cleaning process

Laser Sources [nm]	Power in [dBm]
1531.880	-4.35
1532.350	-1.46
1532.670	-4.69

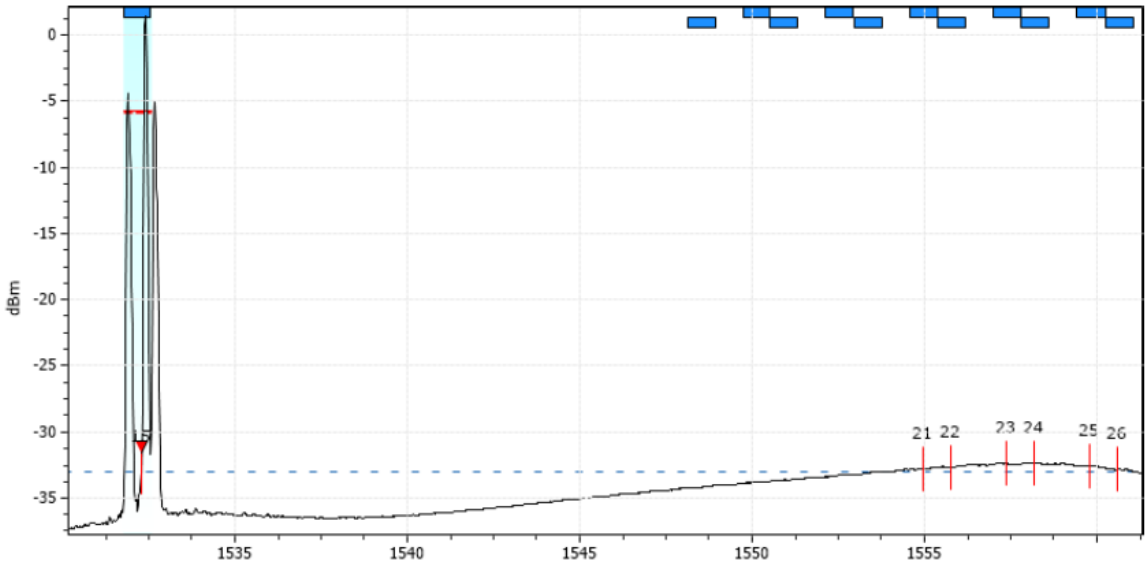

Figure 32 – Input Power at the Fiber

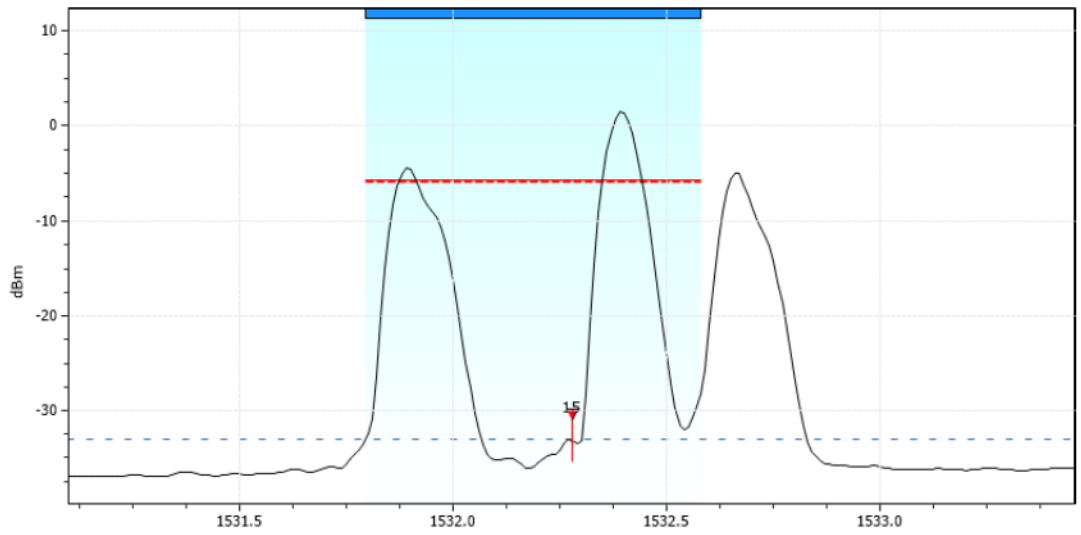

Figure 33 – Initial Input Power and Laser Sources

Proceeding further we connect the fiber and reduce the spacing in order to recreate some side peaks, the initial result was verified in Fig. (4):

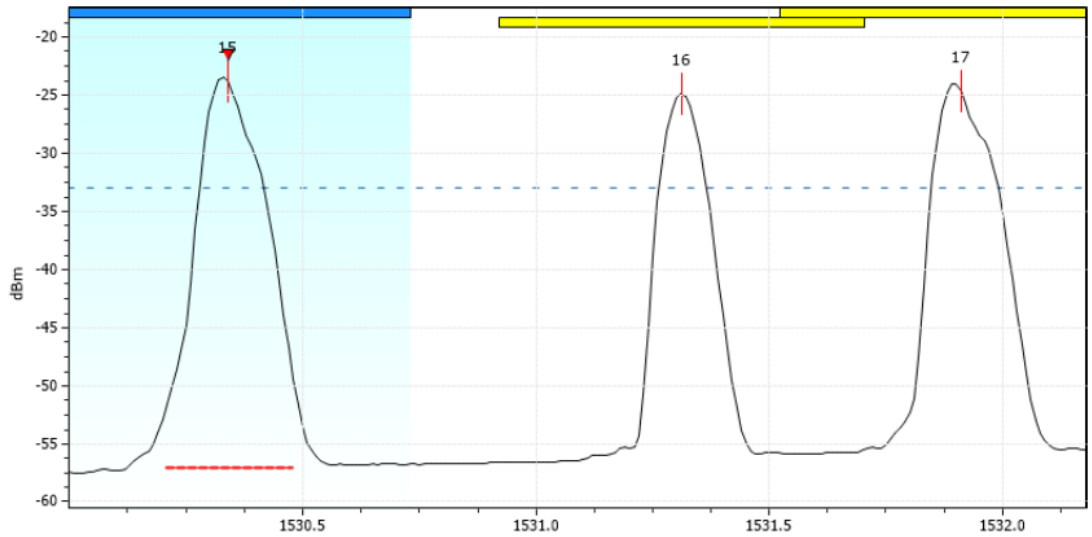

Figure 34 – Initial Non-Degenerated Assessment

The initial evaluation is that, in the construction in general 10dB in power is being loss somewhere in the network, and since all of the laser values dropped in amplitude, one can assume that this loss is occurring after the MUX, and by comparing the power entering the fiber is also safe to assume that the amplification stage is working as expected. After partially eliminating the extrinsic losses the results were:

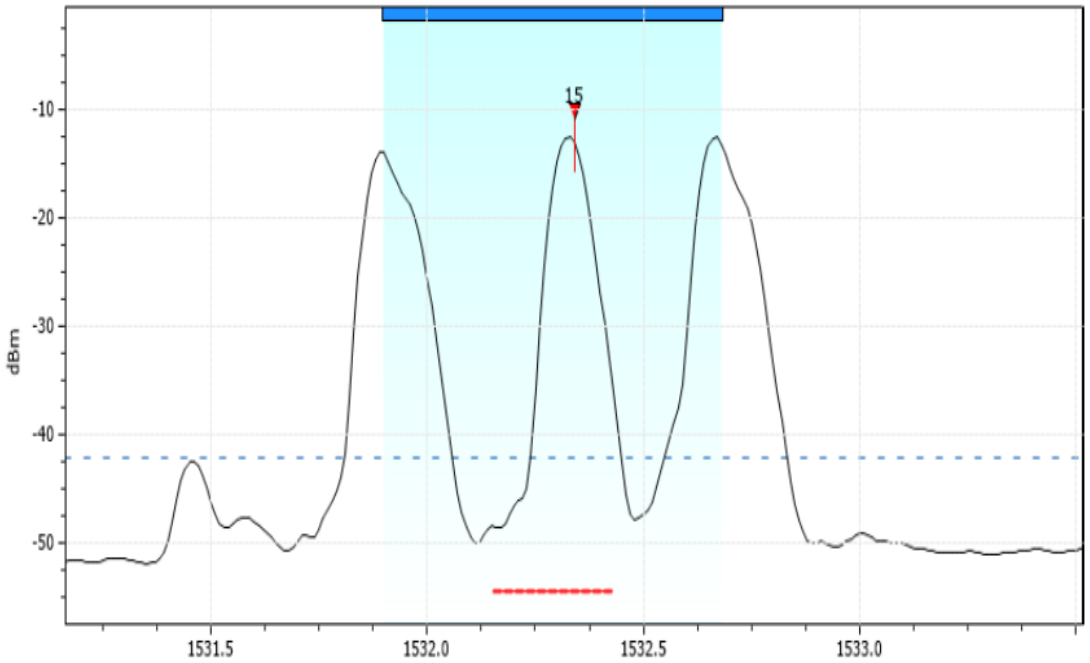

Figure 35 – Non-Degenerated FWM Clean

In figure 5, a large WDM product be can clearly observed at power peak equals to -42.37 dBm marking wavelength at 1531.450 nm this cross product can be calculated from the equation $2y_i - y_k$, where $y_i = 1531.880$ and $y_j = 1532.310$. If applied the formula number (8) we can establish that for 3 laser sources 9 WDM products should be expected, however the remaining WDM products are neglected, hidden or comparable to the level of noise. By increasing the decreasing the channel spacing (changing the tunable laser steps) this was observed:

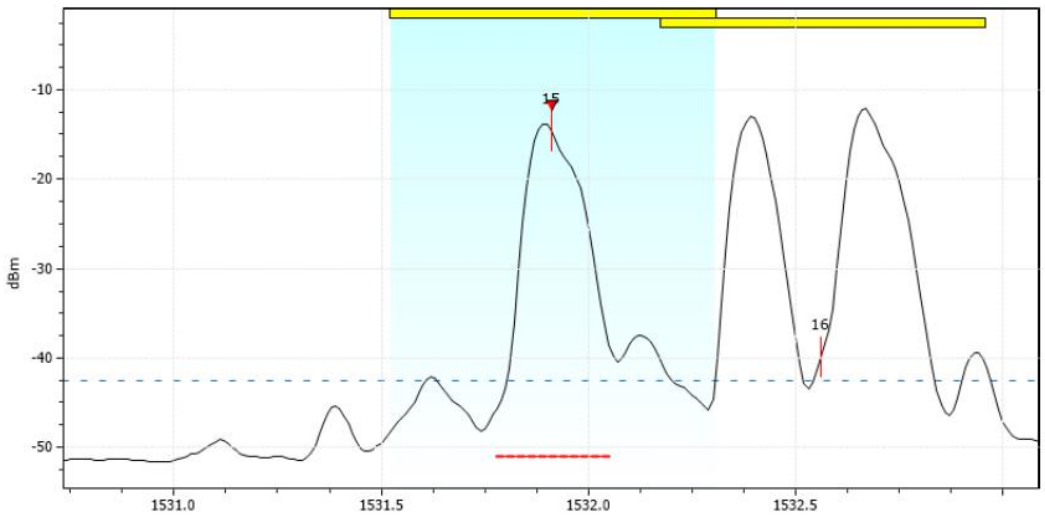

Figure 36 – Non-Degenerated with Peaks

Is clear that by shifting the position of the tunable laser some hidden peaks were uncovered with their respective powers and again we can tune them and predict the FWM product wavelengths:

Table 7 – Predicted Wavelength

WDM products	Laser Sources nm	Equation	Comments
1531.090 nm PW -40.24 dBm	1531.880 (i)	2yi-yk	-13.88 PW dBm
1531.410nm -45,42 dBm	1532.350 (j)	2yi-yj	Tunable – 12.25 pw dBm
1531.560nm Pw -38.71 dBm	1532.670 (k)	yi+yj-yk	-12.36 PW dBm
1532.220nm Pw -35.23 dBm		yi-yj+yk	
1532.992 nm Pw -44.05 dBm		2yk-yj	

Table 8 – Peaks on Figure

WDM products	Laser Sources nm	Comments
1531,130nm PW -49,01	1531,880	-13.88 PW dBm
1531,410nm Pw -45,42	1532.350	Tunable - 12,25 pw dBm
1531,640nm Pw -41,84	1532.670	-12,36 PW dBm
1532,120nm Pw -37,44		
1532,929 nm Pw -39,50		

This experiment was repeated by increasing the power of the tunable laser from 0dbm to -1dBm and the following was observed:

Table 9 – WDM products created with tunable laser equal to -1dBm

WDM products	Laser Sources nm
1531,130nm PW -49,58	1531,880
1531,410nm Pw -43,01	1532.350
1531,640nm Pw -42,06	1532.670
1532,120nm Pw -37,64	
1532,929 nm Pw -40,01	

Is noticeable that the peaks that are further from our laser source are deemed neglectable so the fact that they are increasing with the increase on input power is not relevant, but a conclusion can be reached that smaller input power neglects the effects of the more damaging WDM products since is visible a decrease of power levels when compared to the previous setup, this of course is a single view since we have only two points of comparison.

As mentioned the initially the our EDFA pump is set on the maximum possible value, but the behavior of the overall network and laser peak values without the maximum saturation remained an unsewered question so the next set on this practical chapter was to shift the pump current on our EDFA and observe some of the peaks variation, this resulted in:

Table 10 – WDM Products with EDFA current pump equals to 156.3 mA

WDM products	Laser Sources nm	Comments
1529,350nm Pw -48,24	1530,330	-12.70 PW dBm
	1531,270	Tunable -14.54 PW dBm
	1531,880	-13.69 PW dBm

Table 11 – WDM Products with EDFA current pump equals to 146.3 mA

WDM products	Laser Sources nm	Comments
1529,350nm Pw -49,08	1530,330	-12.93 PW dBm
	1531,270	Tunable -14.85 PW dBm
	1531,880	-14.00 PW dBm

Table 12 – WDM Products with EDFA current pump equals to 136.3 mA

WDM products	Laser Sources nm	Comments
1529,350nm Pw -49,61	1530,330	-12.98 PW dBm
	1531,270	Tunable -14.79 PW dBm
	1531,880	-14.12 PW dBm

Table 13 – WDM Products with EDFA current pump equals to 126.3 mA

WDM products	Laser Sources nm	Comments
1529,350nm Pw -50,24	1530,330	-14.07 PW dBm
	1531,270	Tunable -15.93 PW dBm
	1531,880	-15.13 PW dBm

Table 14 – WDM Products with EDFA current pump equals to 116.3 mA

WDM products	Laser Sources nm	Comments
1529,350nm Pw -50,88	1530,330	-14.71 PW dBm
	1531,270	Tunable -16.78 PW dBm
	1531,880	-16.02 PW dBm

The following progression, when combine with tables 10,11,12,13 and 14 confirms the initial statement that our observed gain is not flat, on its linear regime is decreasing the level of power verified in the output while compared to the input pump decrease the variation does not showcase a 1:1 response.

During this practical experiment an attempt was made in order to showcase the degenerated FWM, the degenerated setup can be achieved by removing one of the SFP modules, leaving the original setup with only 1 tunable laser and a SFP module, after disconnecting the circuit and cleaning and rearranging patch cords the best result is shown in Fig. (37).

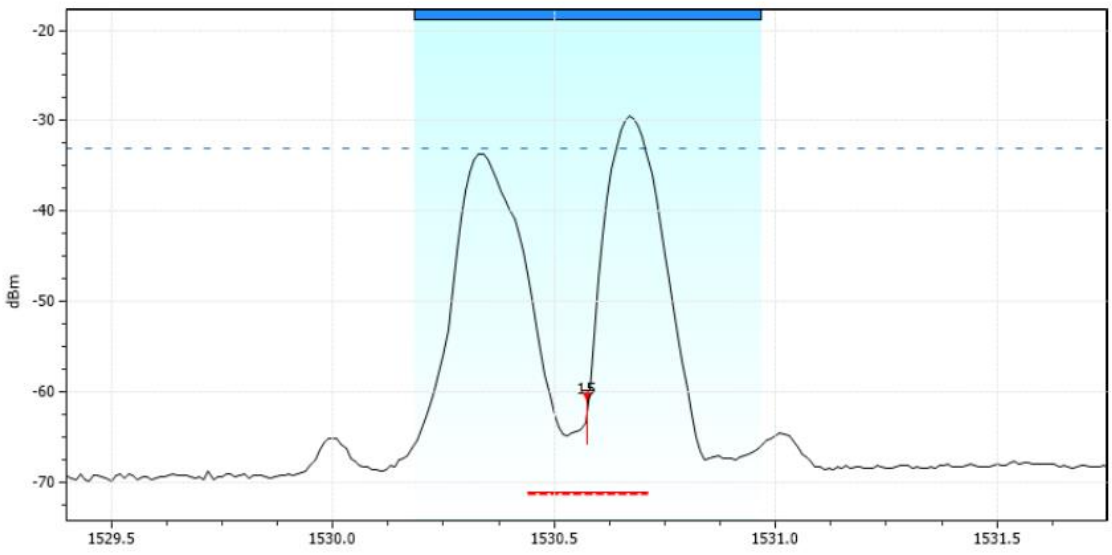

Figure 37 – Degenerated FWM Enhanced

In Fig. (37) we can say that 2 FWM products are visible but are conveniently close to the level of noise, also when compared to the original setup we are observing a drop of almost 20dB lessen within the network, and this prevented the investigation into the degenerated space to proceed further.

Conclusion

Throughout this work, we describe different phenomena that lead to partial or total degradation of the systems transmitted in optical fiber communication systems, with an emphasis on multiple optical channel systems, with the mixture of four waves. In the four-wave mixing, the non-linear effects in the refractive index lead to the formation of new optical wavelengths, some of which are in the range of efficient transmission values in the optical fiber. The inclusion of these new signals results in the degeneration of the original beams, with different consequences addressed in the experimental chapter and in simulations in which it was shown how systems that use dense spacing, being of high demand for greater capacities of the communications links. It was also verified that the mixture of four waves from non-linear processes has a tremendous dependence on the dispersion properties of the optical fiber, the smaller this dispersion, the greater influence is verified between neighboring channels, as seen in Chapter V when a systematic comparison of a fixed length optical link with a range of dispersion values. An analysis was also verified for systems with greater separation between channels considering a common dispersion within the same link as shown in table 3.

As typified in Chapter III there is a significant number of techniques and rules that help in the design and conception of DWDM networks that mitigate the appearance of non-linear effects, failure to comply with these recommendations clearly results in the degradation of the transmitted signal.

In this work it is assumed that the effect of four waves is isolated and occurs in a singular way, when in practice there is a simultaneous occurrence of different non-linear effects which can be considered a topic for future discussions.

The basis of all experiments and simulations was always represented in terms of the optical spectrum and the quality metrics Q-Factor and BER were verified, which indicates that the dimensioning of such networks should include a plan to mitigate these effects. This work is beneficial because it enriches the study of the FWM effect within DWDM networks, in the area of extreme condition on which these systems can operate, on the predicative analysis of their behavior and suppressing techniques. This work can be improved by incorporating other parameters that condition the appearance of this effect such as different modulation schemes, light polarization and others.

For unrelated reasons (illness), it was not possible to complete the series of experiments scheduled for the second week of July, making this work incomplete regarding the number of tasks to be performed, more specifically a correct study of degenerated FWM and the creation of network without the presence of the four-wave mixing effect.

References

[1] G.P. Agrawal,2001, Applications of Nonlinear Fiber Optics, Academic Press, New York, ISBN**:** 9780080499222

[2] Agrawal GP, 2001, Nonlinear Fiber Optics, 3rd Ed., Academic Press, San Diego, CA, ISBN-13: 978-0120451432

[3] Ing. Lucki, Michal, Ph.D. .: lecture notes, presentation: DWDM, CWDM and PON, CTU-FEE in Prague, Dept. of Telecommunication. Available on: https://moodle.fel.cvut.cz/pluginfile.php/187459/course/section/36127/DWDM%20CWDM%20a%20PON.pdf [accessed 04 Feb 2020].

[4] ITU-T: SERIES G: TRANSMISSION SYSTEMS AND MEDIA, DIGITAL SYSTEMS AND NETWORKS Transmission media and optical systems characteristics – Optical fibre cables, Recommendation G.652, Characteristics of a single-mode optical fibre and cable**,** International Telecommunication Union, Geneva, or 2017, available on: https://www.itu.int/rec/T-REC-G.652-201611-I/en [accessed 04 Feb 2020]

[5] Gerson Serra de Almeida, EXPANSÃO DA CAPACIDADE DE TRANSMISSÃO DE SISTEMAS ÓPTICOS ATRAVÉS DA TECNOLOGIA WDM:UM ESTUDO DE CASOS SOBRE O SISTEMA DA ELETRONORTE, , UFPA/ITEC/PPGEE Belém – Pará - Brasil

[6] Timothy K. Cahall and Aharon J. Agranat, 2001, Power balance and wavelength discipline are crucial to the all-optical network, Lightwave. Available on: https://www.lightwaveonline.com/home/article/16668325/power-balance-and-wavelength-discipline-are-crucial-to-the-alloptical-network [accessed 05 Feb 2020]

[7] Bononi, A., Rossi, N., Serena, P., "Transmission Limitations due to Fiber Nonlinearity," Optical Fiber Communication Conference, OSA Technical Digest (Optical Society of America), paper OWO7. 2011.

[8] Li C. (2017) Nonlinear Stimulated Scattering. In: Nonlinear Optics. Springer, Singapore, ISBN 978-981-10-1488-8

[9] PASTORELLI, R. et al. Network planning strategies for next-generation flexible optical networks. Journal of Optical Communications and Networking, 7, n. 3, 2015. A511- A525.

[10] Dr. Rüdiger Paschotta, Cross-Phase Modulation, RP PHOTONICS ENCYCLOPEDIA. Available on: https://www.rp-photonics.com/cross_phase_modulation.html [accessed 15 Feb 2020].

[11] S. P. Singh † and N. Singh, Progress In Electromagnetics Research, PIER 73, 249–275, 2007, Department of Electronics and Communication, University of Allahabad. Available on: http://www.jpier.org/PIER/pier73/13.07040201.Singh.S.pdf [accessed 15 Feb 2020].

[12] Toulose J., Journal of Lightwave Technology IEEE 2005, Optical Nonlinearities in Fibers: Review, Recent Examples, and Systems Applications.

[13] Osamu Aso, Masateru Tadakuma, Shu Namiki, Four Wave mixing in Optical Fiber and its Applications, WP team, Opto Technology Lab., R&D Div.

[14] CARVALHO, H. M. B, 2001, "Efeitos da Polarização na Mistura de Quatro Ondas (FWM) em fibras DS" Dissertação de Mestrado, Dept. Engenharia Elétrica, Unicamp, Campinas, SP.

[15] Robert McMahon, 2001, Nonzero-dispersion-shifted fiber: The choice for DWDM, Lightwave. Available on: https://www.lightwaveonline.com/home/article/16668684/nonzerodispersionshifted-fiber-the-choice-for-dwdm [accessed 21 Feb 2020].

[16] Narottam Das, Optical Communication. Edited. Chapter 10 Realisation of Mixed WDM Transmission Systems ISBN 978-953-51-0784-2, PDF ISBN 978-953-51-6244-5, Published 2012-10-03.

[17] DEEPAK BEHERA, SUMIT VARSHNEY, SUNAINA SRIVASTAVA, AND SWAPNIL TIWARI, 2011, Eye diagram basics: Reading and applying eye diagrams, EDN,Available on: https://www.edn.com/eye-diagram-basics-reading-and-applying-eye-diagrams/ [accessed 04 March 2020].

[18] Ashwin Gumaste, Tony Antony, DWDM Network Designs and Engineering Solutions, Published Dec 13, 2002 by Cisco Press. Part of the Networking Technology series ISBN ISBN-10: 1-58705-074-9

[19] Annasaheb Dange, Advances in Recent Trends in Communication and Networks, College of Engineering and Technology, Ashta, ISBN 9788184245646, 2010, Allied Publishers

[20] IDIL Fibres Optiques, Bank Image, available on: https://www.idil-fibres-optiques.com/product/erbium-doped-fiber/ [accessed 28 July 2020].

[21] TRSRenTelco, Bank Image, available on: https://www.2test.ru/upload/iblock/d73/d73eeb9a082fdf2f9c57ffafe68ea868.pdf [accessed 28 July 2020].

[22] Ilham Rahadi Anshary, 2019, Troubleshooting Problems on Fiber Optic Network Devices of ICON+, Research Gate. Available on: https://www.researchgate.net/figure/SFP-port-on-switch-SFP-module-blue-and-patch-cord-cable_fig2_334459412 [accessed 28 July 2020].

[23] Lightwavestore.com, Fiber/Cable Spools, NZ-DSF Bank Image. Available on: https://www.lightwavestore.com/37-120km-lucent-truewave-rs-fiber-spool-with-2-sc-pc-connectors-with-plastic-film-over-fiber-roll-in-original-full-fiber-length.html [accessed 28 July 2020].